ERDA/JPL - 954144-76/01
Distribution Category UC-63

SILICON RIBBON GROWTH BY A CAPILLARY ACTION SHAPING TECHNIQUE

G. H. Schwuttke, Principal Investigator, 914-897-3140
International Business Machines Corporation
System Products Division, East Fishkill Laboratories
Hopewell Junction, New York 12533

Annual Report
(Quarterly Technical Progress Report Number 4)
June 15, 1976

prepared by
G. H. Schwuttke, T. F. Ciszek, and A. Kran

Under JPL Contract Number: 954144
(Subcontract under NASA Contract NAS7-100)
(Task Order No. RD-152)
Effective Date of Contract: 5/8/75
Contract Expiration Date: 12/31/76

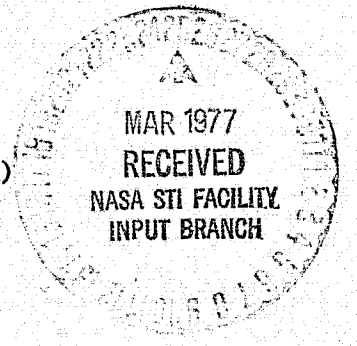

This work was performed for the Jet Propulsion Laboratory, California Institute of Technology, under NASA Contract NAS7-100 for the U.S. Energy Research and Development Administration, Division of Solar Energy.

The JPL Low-Cost Silicon Solar Array Project is funded by ERDA and forms part of the ERDA Photovoltaic Conversion Program to initiate a major effort toward the development of low-cost solar arrays.

CONTENTS

Page

TECHNICAL CONTENT STATEMENT

This report contains information prepared by the International Business Machines Corporation under JPL contract. Its contents are not necessarily endorsed by the Jet Propulsion Laboratory, California Institute of Technology, or by the National Aeronautics and Space Administration.

RESEARCH PROGRAM PLAN

OBJECTIVES

1. Technological assessment of ribbon growth of silicon by a capillary action shaping technique.

2. Economic evaluation of ribbon silicon grown by a capillary action shaping technique as low-cost silicon.

SYNOPSIS OF PROGRAM OF STUDY

1. Crystal growth of silicon ribbons.

2. Characterization of silicon ribbons.

3. Economic evaluations and computer-aided simulation of ribbon growth.

FOURTH QUARTER HIGHLIGHTS

- A new capillary action shaping technique die was designed. This new die allows improvements in surface smoothness and in SiC surface-particle density.

- Forty-seven ribbons greater than 0.5 meter long and 25 mm wide were grown during the last quarter.

- Ribbon width was extended to 38 mm (1 1/2 inches).

- Surface films on ribbon surfaces were analyzed as SiC crystallites. Significant structural differences, depending on the deposition location, were found.

- Epitaxial growth of SiC through preferential incorporation of (111) SiC planes parallel to (111) silicon planes was identified as an important mechanism for surface film formation.

- Development of a new technology-forecasting technique was continued. This technique is being applied to projecting the future cost of energy at the level of silicon-sheet material. From a baseline, future technology capability is projected through full

maturity. The concept of chronology is introduced by estimating the probability of meeting the objective associated with the production-unit parameter and leads to a specific cost-versus-time relationship.

- Silicon-sheet technology was shown to have the potential for achieving future low-cost material objectives for photovoltaic applications, if development milestones defined in this study are met.

- 1980 and 1985 energy-capacity costs of $750/kWE and $350/kWE, respectively, at the level of silicon-sheet material, are projected.

- This analysis confirmed, from a silicon-sheet material standpoint, that ERDA-stated energy-capacity cost objectives at the array level are achievable, but with little margin for error.

CRYSTAL GROWTH

by

T. F. Ciszek

1. INTRODUCTION

The crystal-growth method under investigation is a capillary action shaping technique. Meniscus shaping for the desired ribbon geometry occurs at the vertex of a wettable die. As ribbon growth depletes the melt meniscus, capillary action supplies replacement material. The configuration of the technique used in our initial studies is shown in Fig. 1 and is similar to the edge-defined, film-fed growth (EFG) process described by LaBelle (1). The crystal-growth method has been applied to silicon ribbons for several years (2,3,4), and long ribbons up to 25 mm in width have been produced.

Certain problems still await solution before the technique becomes viable for large-scale economical photovoltaic applications. High-density graphite fulfills the durability and wettability requirements of a die (2) and has been used, to date, for most silicon ribbon growth; it is not, however, completely non-reactive. Good crystallographic perfection has been achieved on small ribbon segments (2,3), but the

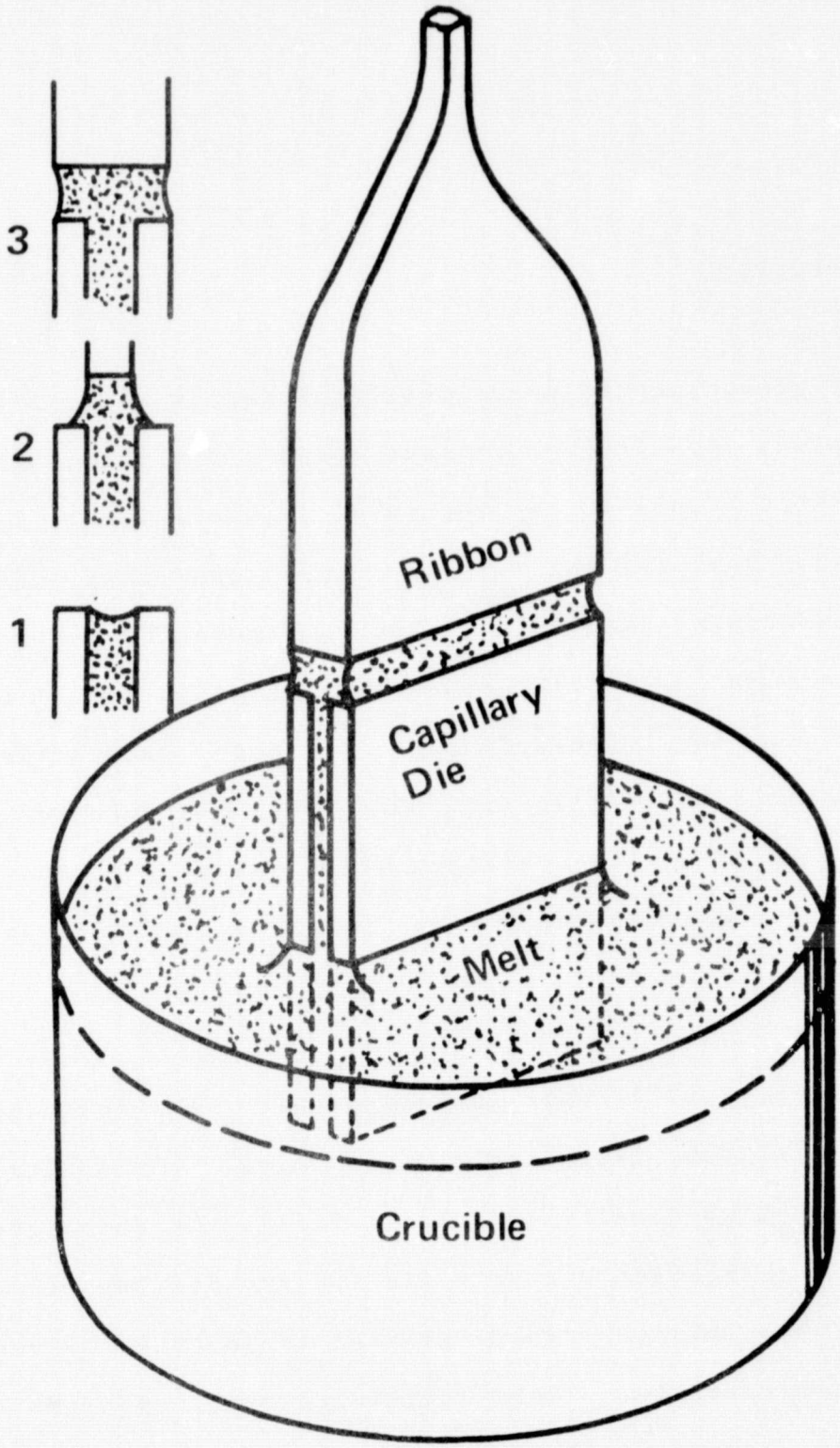

Fig. 1. A schematic diagram of the capillary action shaping technique for silicon ribbon growth.

structure of large ribbons is marred by planar, line, and point defects. Our objective in this work is to attain a clear technological assessment of silicon ribbon growth by the capillary action shaping technique and to enhance the applicability of the technique to photovoltaic power device material.

In this report, a new capillary die design is described. It represents a departure from the die types used for edge-defined, film-fed growth, in that the bounding edges of the die top are not parallel or concentric with the growing ribbon. The new dies allow a higher melt meniscus with concomitant improvements in surface smoothness and freedom from SiC surface particles, which can degrade perfection.

Also in this reporting period, ribbons were grown for delivery to JPL. Twenty ribbons and 30 ribbon samples were shipped. Detailed dimensional characteristics of most ribbons grown during the past year are presented in Appendix 1.

Finally, our initial progress in the growth of 38-mm (1-1/2-inch)-wide ribbons, up to 46 cm in length, is reported.

2. CAPILLARY ACTION SHAPING TECHNIQUE

DIE DESIGN CONSIDERATIONS

The capillary die design used for meniscus shaping in our capillary action shaping technique of ribbon growth over the past several months is indicated in Fig. 2. The die is a departure from the edge-defined, film-fed technique of crystal growth, in that the cross section of the growing ribbon is not concentric with the top edges of the die. The die top is considerably thicker in the mid-region than at the edges, yet the resultant ribbon is flat or somewhat

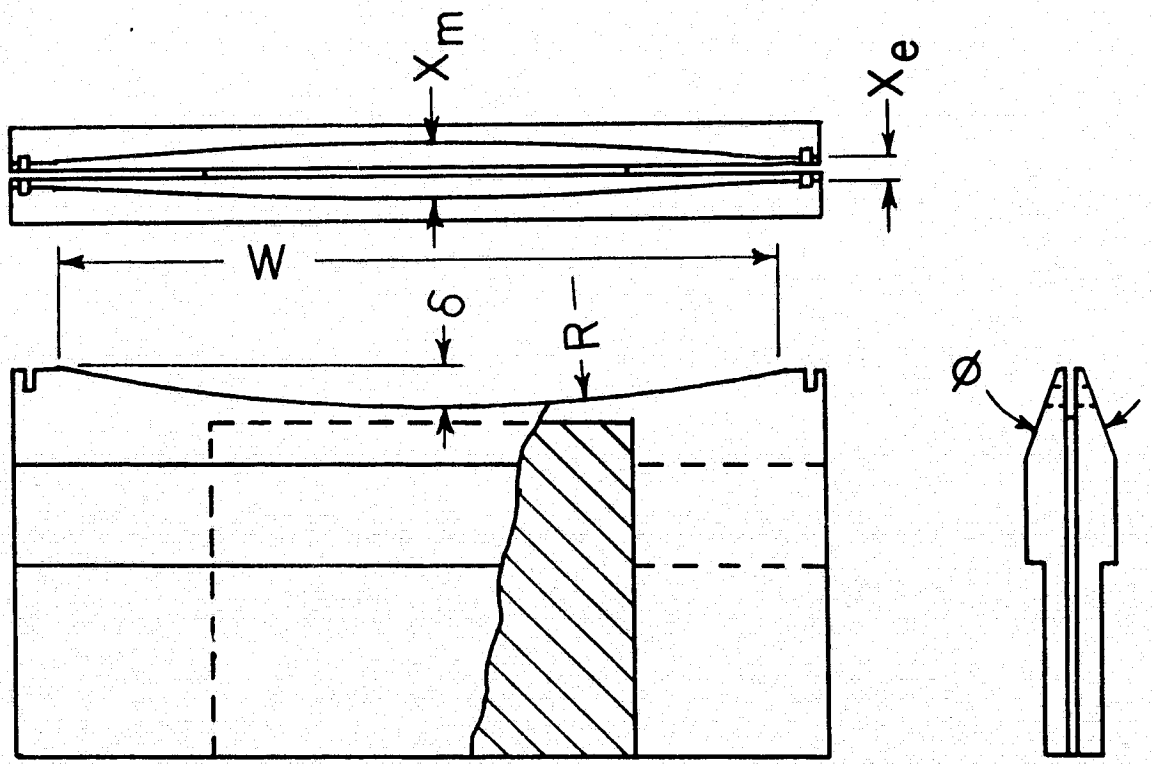

Fig. 2. Die for improved capillary action shaping technique ribbon growth.

thicker at the edges than in the middle. This die design allows a higher meniscus at the central region of the solidification front and thus reduces problems which can occur when using flat-top dies or curved-top dies with parallel top edges as in the EFG technique. Such problems come about primarily from the fact that the graphite die used for silicon growth slowly dissolves in the liquid. Carbon-saturated silicon rises up the capillary slot in the die and comes to the top region where ribbon solidification occurs. This top region is the coolest region in the growth system. Here, excess carbon is forced out of the saturated silicon solution in the form of β-SiC crystallites, which tend to collect at the top surface of the die. These crystallites distort the melt meniscus and make the ribbon non-uniform in its surface smoothness. Because of the proximity of the freezing interface to the die top, the SiC particles are frequently incorporated in the ribbon, where they generate dislocations and other defects.

It is advantageous to keep the interface of the freezing ribbon as far as possible from the die top, and this can be accomplished with the structure shown in Fig. 2. The die top surface is curved so that it is higher at the edges than in the middle. In this way, if the ribbon's solid-liquid interface is maintained approximately planar, then the

interface is further from the die, at least in the central region. The central region is most critical for generation of defects in the silicon body. However, if the width of the die top is kept constant while the die top surface is curved, then a higher meniscus in the central region necessarily implies that the top of the meniscus is thinner there. This would cause the ribbon to be very non-uniform in thickness from one edge to the other (i.e., much thinner in the middle than at the ends). Thus, not only should the die top curve downward from the ends toward the central region, but it must also become wider in the central region than at the ends, as in Fig. 2. The meniscus, then, has a wider base in the central region. The wider base, combined with the greater meniscus height in the central region, results in a more uniform thickness at the solid-liquid interface. In summary, there are two things that are important to the die design: one is the curvature of the top surface, and the other is the widening of the die top in the central region.

Figure 3 is a cross section at the center of the die before the seed crystal is applied. No through capillary is shown because this is the area that holds the two major portions of the die together. Figure 3b shows the edge condition with the ribbon in place, and Figure 3c is a vertical cross

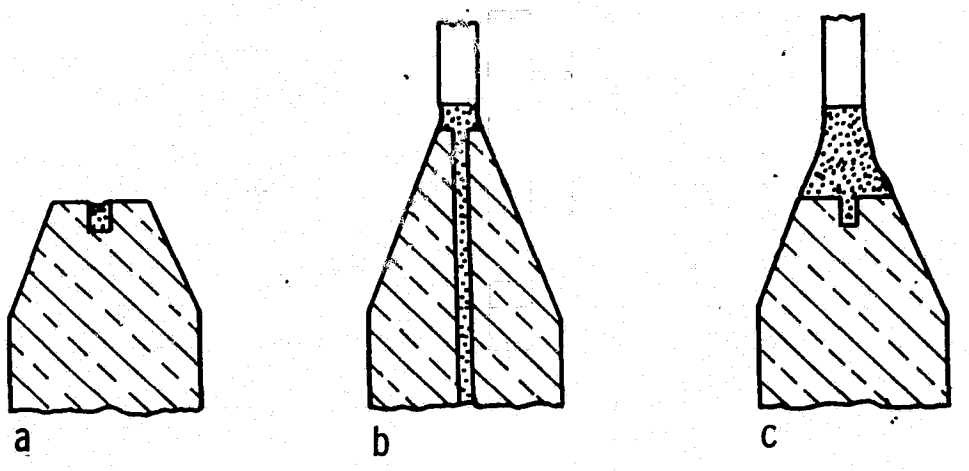

Fig. 3. Cross section through die and ribbon: (a) central die top before seeding, (b) near edge of die during growth, and (c) near central region of die top during growth.

section through the central region during full-width ribbon growth. It can be seen that, even though the top of the die is narrow at the ends and relatively wide in the middle, the ribbon thickness is essentially uniform because the freezing interface is close to the die top near the ends of the die, but higher above the die top near the middle. The top of the meniscus is about as wide as the bottom of the meniscus at the end areas (Fig. 3b). However, the cross section of the meniscus near the central point of the die and ribbon (Fig. 3c) tapers from a wide base to a narrow top. By proper choice of the curvature of the die top and the taper angle of the sides of the die, an optimum value for this variation of the width of the die top with position along the die top can be obtained.

The outer edges of the top die surface, that is, those edges which bound the lower portion of the melt meniscus from which the ribbon solidifies, can be considered to be determined by the intersection of a vertical truncated wedge with enclosed angle- ϕ, truncated thickness - X_e, and width - W, with a horizontal cylinder of radius R. The intersection is made essentially such that the cylindrical surface contains the short edges, X_e, of the wedge top. The resultant die top is that of Fig. 2, where X_e is the top surface thickness at the ends, X_m the top surface thickness in the center, ϕ the enclosed angle of the tapered wedge, R the radius of curvature of the top surface, W the width of the die, and δ the difference in height from ends to center. The top of the die, thus, smoothly increases in thickness from X_e to X_m and decreases in height, by an amount δ, as we go from the die edge to the die middle.

The objective in this design is to attain a high-melt meniscus in the central region, since proximity of the freezing interface to the die top is detrimental to ribbon perfection and surface smoothness, while still maintaining the proximity at the die ends to stabilize the ribbon width. Furthermore, this must be achieved in a smooth transition to facilitate the early stages of growth from seed size to full width.

R and ϕ are chosen to optimize the values of $X_m - X_e$ and δ for successful ribbon growth. These parameters are given by

$$\delta = R - \frac{W}{2 \tan (\sin^{-1} \frac{W}{2R})}$$

$$X_m - X_e = 2 \delta \tan \phi / 2.$$

For the 25-mm-wide ribbons grown recently, dies were constructed with R=101.6 mm, ϕ =40°, and X_e =0.54 mm. Thus, X_m was $\sim$0.99 mm. The typical edge thickness and middle thickness of the resultant ribbons were 0.42 mm and 0.21 mm, respectively; the exact values were dependent upon growth rate. Better surface smoothness and a lower SiC surface-particle density ($< 0.1/cm^2$) were seen previously with slightly thicker dies, where X_e was 0.79 mm and R and ϕ were as above. These ribbons had a typical edge thickness of 0.64 mm and a middle thickness of 0.42 mm. The thickness of the die top in the central region was 1.37 mm in this case. Although these ribbons have a relatively large deviation from flatness (on the order of 0.1 mm), with the edges being thicker than the middle, they are quite smooth on a local scale compared with ribbons grown from an EFG die, as was shown in Fig. 7 of the second quarterly report (5). Local roughness variations of 10-μm maximum amplitude have been achieved with the new die design, whereas roughness variations of about 50-μm maximum

amplitude were typical with the flat top die. Silicon carbide particle densities with the new die are typically $<0.1/cm^2$ as compared with $5/cm^2$ for the EFG die.

During this quarter, 25-mm-wide dies with the dimensions indicated above were used in conjunction with our standard growth setup [see pp.7-9 of the third quarterly report (6)] to grow ribbons for delivery to JPL. Forty-seven ribbons, corresponding to a total length of 24 m, were grown. The average length was 0.51 m, the average edge thickness was 0.41 mm, and the average central thickness was 0.27 mm. Twenty complete ribbons and 30 ribbon segments were shipped to JPL. Ribbons as thin as 0.30 mm at the edge and 0.10 mm in the central region were produced when pull speeds in excess of 3 cm/min were employed. However, these ribbons exhibited a non-flat surface, with undulating bulges of small amplitude. In general, surface roughness, SiC particle density, asymmetrical growth, and growth-control requirements were all more severe with dies designed for thin ribbon growth than with dies designed for thicker ribbon growth.

Twelve meters of ribbon were grown from a single die in 9 melt-down cycles. The die still appeared to be serviceable at this point, although ribbon roughness had increased somewhat because of SiC buildup at the die top.

3. GROWTH OF 38-MM-WIDE RIBBONS

The concepts discussed relative to 25-mm-wide capillary action shaping technique dies were extended to the design of a die for 38-mm (1-1/2-inch)-wide ribbons. In this die, δ = 1.0 mm, ϕ = 50°, X_e = 0.44, and X_m = 1.16 mm. Three full-width ribbons were grown, the longest of which was 46 cm at full (38-mm) width (see Fig. 4). The ribbons were grown at speeds of 16-18 mm/min. Typically, the edge thickness was 0.42 mm and the middle thickness was 0.54 mm. A thinner portion (0.37 mm) was present, however, between the edge and the middle. Thus the total deviation from flatness was about 0.09 mm. More difficulty was noticed with freeze-out during the process of spreading from seed-width (3-mm) to full-width growth than had been observed during 25-mm-wide ribbon growth. Dies are being fabricated with slightly different dimensional parameters, in hopes of reducing this problem.

The crystallographic defect structure and surface smoothness of the 38-mm-wide ribbons are similar to those seen for 25-mm-wide ribbons. The largest ribbon grown (3.8 cm x 46 cm) had a SiC surface-particle density of 0.07/cm^2, which is also comparable to densities seen with 25-mm-wide ribbons.

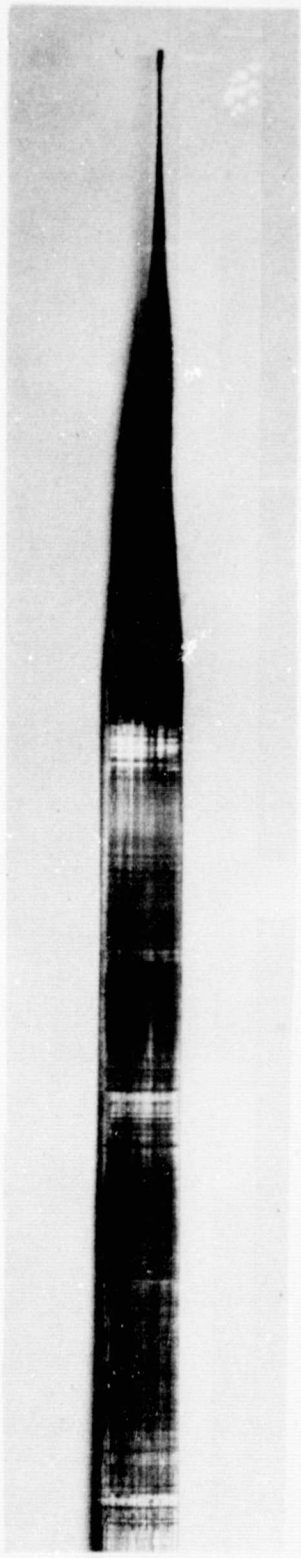

Fig. 4. A 38-mm-wide by 46-cm-long silicon ribbon grown by the capillary action shaping technique.

4. REFERENCES

1. H. E. LaBelle, Jr., Mater. Res. Bull. 6, 581 (1971).

2. T. F. Ciszek, Mater. Res. Bull. 7, 731 (1972).

3. T. F. Ciszek and G. H. Schwuttke, Phys. Status Solidi (a) 27, 231 (1975).

4. J. C. Swartz, T. Surek, and B. Chalmers, J. Electron. Mater. 4, 255 (1975).

5. Quarterly Technical Progress Report Number 2, JPL Contract 954144, G. H. Schwuttke, Principal Investigator, December 15, 1975.

6. Quarterly Technical Progress Report Number 3, JPL Contract 954144, G. H. Schwuttke, Principal Investigator, March 15, 1976.

5. ACKNOWLEDGMENT

Technical support in crystal growing was provided by F. Newman.

Appendix 1

DIMENSIONAL CHARACTERISTICS OF SOME RIBBONS GROWN DURING AUGUST 1975 - MAY 1976

Ribbon Run No.	Seed Orientation Axis	Seed Orientation Surface	Usable Length (cm)	Width (mm) Max	Width (mm) Min	Thickness (mm) Seed Max	Thickness (mm) Seed Min	Thickness (mm) Tail Max	Thickness (mm) Tail Min
50805	0	0	38	8.6	6.7	1.01	.00	1.03	.00
50806	0	0	65	8.1	6.2	1.00	.00	1.05	.00
50807	0	0	25	8.7	7.6	1.10	.00	1.15	.00
50808	0	0	34	8.4	8.1	1.06	.00	1.21	.00
50809	0	0	114	7.3	6.7	1.01	.00	1.05	.00
50811	0	0	28	8.0	7.1	1.35	.00	1.35	.00
50825	0	0	32	4.7	4.2	1.58	.00	1.60	.00
50826	0	0	32	5.5	3.8	1.25	.00	1.43	.00
50909	0	0	23	26.2	25.8	.70	.35	.67	.39
50911	110	111	24	25.7	24.4	.65	.35	.62	.41
50916	110	100	46	26.0	.0	.73	.54	.62	.33
50919	110	100	90	26.0	.0	.55	.23	.65	.36
50926	110	100	18	26.0	.0	.65	.57	.65	.56
50927	110	100	40	26.0	.0	.53	.40	.54	.34
50928	110	100	45	26.0	.0	.49	.32	.50	.31
51003	110	112	49	25.6	23.6	.67	.51	.63	.46
51005	110	112	50	26.1	24.7	.63	.44	.66	.45
51007	110	112	51	26.4	23.0	.75	.53	.73	.45
51008	110	112	44	25.6	23.7	.63	.40	.66	.43
51012	100	110	91	25.9	24.3	.69	.49	.68	.47
51013	100	110	20	26.0	25.0	.64	.42	.68	.51
51014	100	110	54	25.7	21.2	.69	.62	.62	.34
51015	110	100	84	25.1	23.4	.61	.35	.64	.34
51016	110	100	52	24.8	17.0	.73	.48	.60	.39
51017	110	100	22	24.7	23.8	.64	.45	.44	.26
51018	110	100	23	25.1	25.0	.72	.43	.67	.41
51019	110	100	56	25.0	23.6	.67	.44	.55	.35
51021	110	100	54	26.2	24.4	.65	.49	.66	.38
51022	110	100	63	25.6	23.8	.63	.38	.59	.28
51023	110	100	63	25.5	24.1	.62	.35	.59	.39
51024	110	100	24	26.2	12.5	.63	.35	.64	.26
51025	110	100	58	25.7	23.3	.54	.31	.56	.22
51026	110	100	62	25.4	24.6	.62	.42	.62	.37
51027	110	100	59	24.9	24.5	.51	.29	.52	.26
51102	110	112	12	.0	.0	.00	.00	.00	.00
51104	110	100	59	25.3	23.5	.54	.40	.51	.36

Ribbon Run No.	Seed Orientation Axis	Seed Orientation Surface	Usable Length (cm)	Width (mm) Max	Width (mm) Min	Thickness (mm) Seed Max	Thickness (mm) Seed Min	Thickness (mm) Tail Max	Thickness (mm) Tail Min
51107	110	112	49	25.5	24.1	.45	.29	.50	.28
51110	110	100	10	25.7	23.3	.55	.50	.55	.50
51114	110	100	48	25.4	24.4	.50	.36	.50	.34
51115	110	100	87	25.6	25.2	.46	.30	.57	.35
51118	110	100	57	25.2	24.8	.46	.31	.45	.29
51119	110	100	54	24.7	24.5	.43	.28	.46	.29
51120	110	100	21	24.9	23.8	.45	.32	.47	.25
51201	110	100	16	24.6	17.4	.47	.50	.50	.35
51202	110	100	60	25.0	24.1	.52	.42	.50	.45
51203	110	100	19	25.5	24.1	.76	.50	.45	.36
51205	110	100	36	25.0	24.9	.55	.45	.50	.45
51207	110	100	20	24.5	22.2	.61	.40	.26	.22
51208	110	100	46	24.6	24.3	.50	.40	.46	.36
51209	110	112	53	.0	.0	.45	.35	.00	.00
51210	110	112	46	24.9	20.6	.67	.50	.65	.50
51213	110	112	32	23.5	14.0	.38	.32	.53	.40
51214	110	100	55	24.8	23.2	.48	.40	.45	.41
51216	110	100	39	25.3	22.7	.71	.52	.73	.45
51217	110	100	57	24.7	23.4	.74	.48	.75	.47
51218	110	100	45	22.9	22.4	.55	.50	.60	.50
60102	110	100	56	25.5	24.9	.53	.39	.50	.33
60103	110	100	51	25.2	24.2	.48	.31	.45	.27
60104	110	112	60	25.4	24.3	.49	.29	.52	.33
60105	110	100	58	24.9	18.8	.50	.45	.50	.45
60110	110	100	46	24.8	23.6	.53	.42	.50	.37
60111	110	100	94	25.4	23.8	.00	.00	.00	.00
60112	110	100	90	24.9	23.4	.45	.35	.50	.27
60114	110	100	33	25.4	22.7	.50	.45	.53	.36
60115	110	100	36	25.2	20.1	.50	.40	.40	.30
60116	110	100	31	25.2	22.4	.53	.42	.37	.28
60119	110	100	28	25.4	25.1	.55	.50	.54	.38
60120	110	100	95	.0	.0	.00	.00	.00	.00
60202	110	100	96	24.6	23.7	.50	.32	.47	.30
60203	110	100	25	25.5	22.2	.57	.38	.55	.25
60206	110	100	9	23.1	18.1	.62	.70	.60	.64
60209	110	100	45	25.9	24.2	.80	.90	.64	.90
60212	110	111	55	25.7	25.1	.60	.50	.60	.40
60213	110	111	77	25.6	25.4	.60	.85	.00	.00
60216	110	100	40	24.6	24.2	.70	.80	.55	.65
60217	110	100	18	24.4	24.2	.60	.85	.42	.52
60303	110	111	55	24.9	22.5	.47	.43	.45	.35
60304	100	110	55	25.5	22.6	.45	.42	.42	.22
60309	100	110	53	25.6	23.4	.47	.50	.42	.45
60310	100	110	23	25.2	23.9	.35	.35	.38	.40
60312	111	110	41	24.7	21.7	.32	.32	.35	.37
60318	100	110	44	25.6	23.7	.44	.40	.45	.37
60320	100	110	55	25.3	24.3	.42	.38	.36	.30
60322	111	112	57	24.7	24.0	.40	.34	.41	.25

Ribbon Run No.	Seed Orientation Axis	Seed Orientation Surface	Usable Length (cm)	Width (mm) Max	Width (mm) Min	Thickness (mm) Seed Max	Thickness (mm) Seed Min	Thickness (mm) Tail Max	Thickness (mm) Tail Min
60323	111	112	29	24.6	22.0	.30	.27	.32	.22
60324	111	112	54	24.4	22.2	.35	.28	.32	.24
60325	110	100	18	23.9	18.6	.65	.70	.50	.40
60326	110	100	38	25.5	21.9	.45	.38	.54	.46
60328	110	100	35	25.3	25.0	.45	.42	.40	.28
60329	110	112	56	24.8	22.7	.30	.25	.40	.28
60330	110	112	43	25.4	24.7	.30	.26	.38	.30
60337	100	110	52	25.2	18.0	.40	.27	.50	.22
60341	100	110	55	25.1	23.7	.40	.35	.48	.32
60401	100	110	56	26.2	25.8	.50	.35	.50	.37
60402	100	110	57	25.7	25.2	.45	.32	.45	.30
60404	110	100	76	26.4	24.6	.40	.21	.50	.32
60406	100	110	56	25.8	25.0	.52	.36	.52	.24
60407	100	110	56	.0	.0	.00	.00	.00	.00
60408	100	110	56	25.0	24.2	.30	.16	.30	.15
60409	100	110	48	24.8	23.7	.30	.15	.35	.10
60414	110	100	56	25.6	25.0	.45	.25	.35	.20
60416	100	110	58	25.4	23.6	.45	.22	.38	.18
60418	121	111	54	25.4	20.5	.45	.22	.35	.10
60419	121	111	56	25.2	24.5	.40	.22	.32	.10
60420	121	111	32	25.2	25.0	.32	.19	.35	.15
60421	121	101	50	25.2	22.4	.48	.37	.48	.32
60422	121	101	52	25.0	23.1	.45	.25	.43	.25
60432	100	110	55	24.9	24.7	.40	.30	.00	.00
60436	100	110	52	24.8	24.1	.48	.41	.00	.00
60437	121	111	55	25.2	24.1	.40	.28	.45	.32
60438	121	111	43	25.0	22.9	.35	.23	.28	.18
60439	121	111	54	25.5	24.1	.45	.29	.42	.30
60440	121	111	56	24.5	24.3	.40	.25	.39	.24
60442	121	111	16	24.4	23.1	.42	.27	.42	.25
60443	121	111	38	24.3	20.5	.40	.32	.36	.16
60444	121	111	39	24.4	24.3	.42	.19	.45	.20
60446	100	110	56	24.4	17.2	.38	.25	.38	.22
60447	121	111	58	24.6	19.7	.35	.19	.45	.21
60448	121	101	53	24.4	24.1	.45	.20	.40	.15
60506	100	110	46	38.2	37.8	.55	.65	.50	.65
60511	110	112	36	39.2	37.4	.43	.55	.44	.53
60520	110	112	58	25.2	25.0	.52	.45	.51	.45
60521	121	101	91	24.7	22.7	.40	.38	.40	.28
60522	110	112	90	25.2	24.8	.40	.35	.45	.28
60523	110	112	63	24.7	24.5	.42	.30	.39	.30
60525	121	101	55	24.7	24.6	.45	.40	.45	.40
60526	110	112	58	24.6	23.3	.40	.20	.40	.25
60527	110	112	81	25.0	24.3	.40	.20	.50	.25

A 0.0 ENTRY INDICATES NO MEASUREMENT WAS MADE.

ANALYSIS OF VAPOR-DEPOSITED SILICON CARBIDE FILMS ON SILICON RIBBON SURFACES

by

K. H. Yang and G. H. Schwuttke

1. INTRODUCTION

The growth of perfect single-crystal silicon ribbons through the capillary action shaping technique by use of carbon dies is complicated by the formation of SiC during ribbon growth. As shown in the first quarterly report (1), frequently, small SiC crystals form in the orifice of the die. The carbide growth is the result of liquid transport of dissolved carbon from hot regions - submersed die - where the equilibrium carbon concentration is relatively high to the cold regions - die top - where it is lower. Thus a carbon supersaturation occurs at the die top. This supersaturation at the die top is enhanced through carbon rejection at the growth interface and is relieved through carbide growth. Sometimes, crystallites get detached from the die and float in the meniscus at the top of the die. Frequently, small crystals attach to the silicon ribbon during growth, thus destroying the perfection of the crystal.

This report draws attention to a second mechanism operative in the formation of unwanted SiC crystals. This mechanism is based on SiC formation on the ribbon surface via vapor transport deposition. Vapor-phase deposition of SiC is particularly active during the seeding phase and during the initial growth period, leading to a more or less dense SiC film on the ribbon surface. Such SiC films influence destructively the efficiency of ribbon solar cells. To minimize film formation it is important to understand the crystallographic nature of the film as well as its mechanism of growth. This report relates to these problems and presents a complete analysis of such films.

2. ANALYSIS OF SURFACE FILMS ON RIBBONS

Visual inspection of seed-ribbon crystals as grown reveals that the seed is covered with a dull bluish film while the surface of the ribbon close to the interface looks dull and dark. The surface dullness decreases rapidly with the distance from the interface, and a shiny ribbon surface is normally obtained after 10 cm of ribbon growth. The surface film formation is more pronounced for lower growth speeds and very strong during the seeding operation because of the longer residence time of the seed. In the following, such surface films on ribbons are analyzed through optical and electron transmission microscopy.

3. OPTICAL MICROSCOPY OF SURFACE FILMS

The variation of surface-film morphology with distance s from the seed-ribbon interface is shown in the photomicrographs of Figs. 1a to 1f. Figures 1a and 1b show the film structure on the seed and on the ribbon, above and below the interface. No particular features are resolved optically. The film covers the silicon surface completely. With increasing distance from the interface, the ribbon surface is covered less completely and the optical microscope reveals well-developed dendritic crystal structures covering the ribbon surface. The number of dendrites on the ribbon surface decreases rapidly with increasing distance s from the interface. Note the preferential nucleation of dendrites in grain boundaries, shown in Figs. 1d and 1e. Twin boundaries do not act as preferential nucleation sites, shown in Fig. 1f. Single isolated dendrites may form during successive ribbon growth, particularly if a change in growth speed occurs.

4. TRANSMISSION ELECTRON MICROSCOPY OF SURFACE FILMS

Optical microscopy cannot identify the crystallographic nature of the films. Therefore, a transmission electron

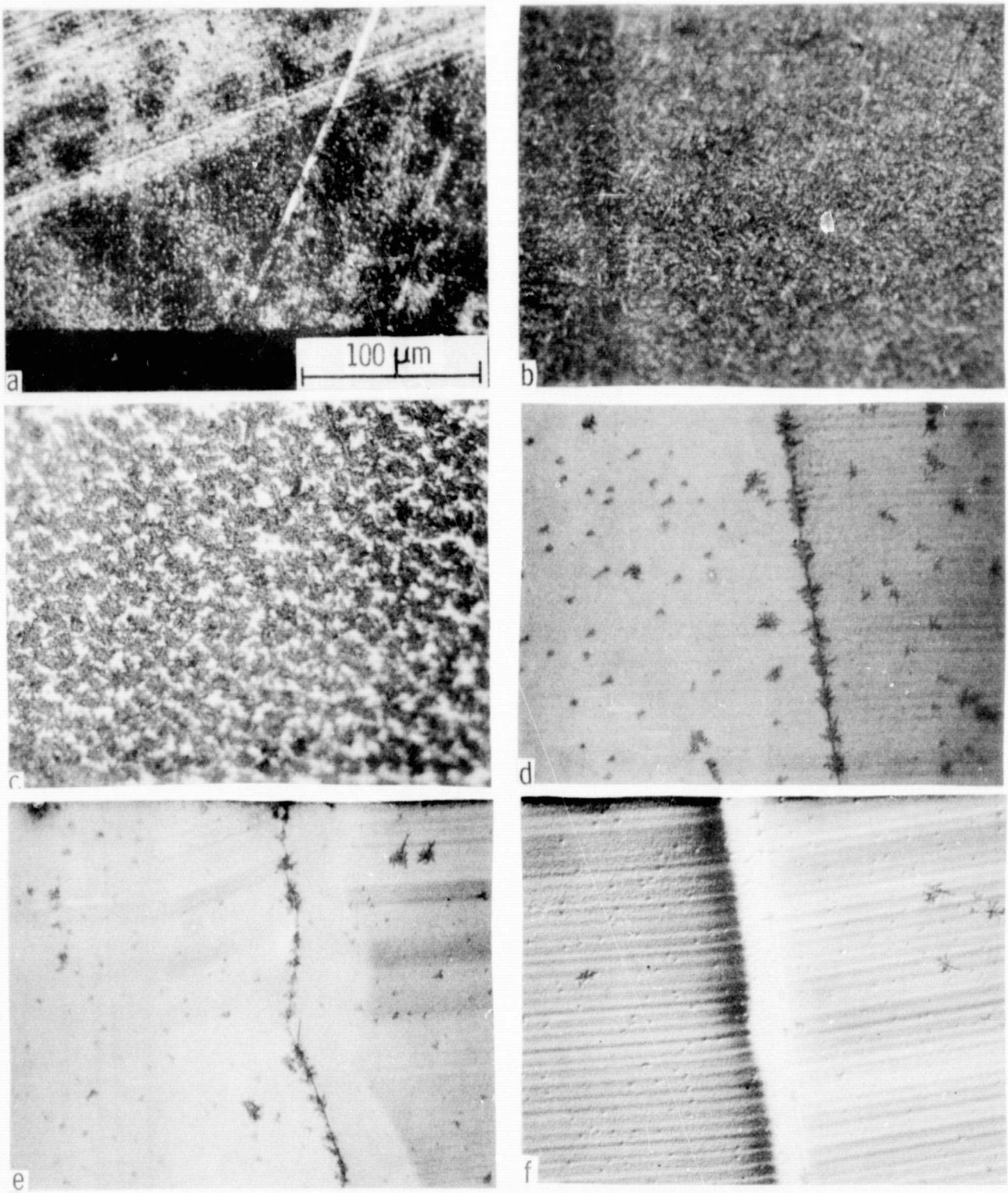

Fig. 1. Optical micrographs showing (a) β-SiC film on seed surface, (b) unresolvable morphology of dull surface at s $\approx$ 2 mm, well-defined dendrites, (c) at s $\approx$ 1 cm, (d) at s $\approx$ 7 cm, (e) at s $\approx$ 10 cm, and (f) at s $\approx$ 20 cm. Note that the density of dendrites decreases with increasing s.

microscopy analysis was made. For this purpose, 3-mm-diameter specimens were cut ultrasonically out of seed and ribbon crystals at different locations. The specimens were jet-etched, using a mixture of HNO_3/HF. Before etching, the specimens were thinned by mechanical lapping (on one side only), mainly for film removal. Subsequently, the jet etch was applied to the lapped side until the specimen was thin enough for electron beam penetration. It was noted that the surface film was very resistant to the etch. Consequently, it was easy to etch holes into the silicon and thus isolate the film for transmission electron microscopy work. Figure 2 shows some typical results for the films covering the seed section. Figure 2a is a transmission electron micrograph of a seed specimen. Note the square structure of the silicon holes typical for the (100) orientation of the seed face. Figure 2b is the corresponding electron diffraction pattern, and Fig. 2c gives the aperture-limited dark-field picture obtained at position A indicated in Fig. 2b. The diffraction pattern (Fig. 2b) is analyzed as β-SiC. The results are summarized in Table I. The dark-field analysis (Fig. 2c) indicates that the film consists of randomly oriented crystallites. The size of these crystallites ranges approximately from 700 to 1500 Å.

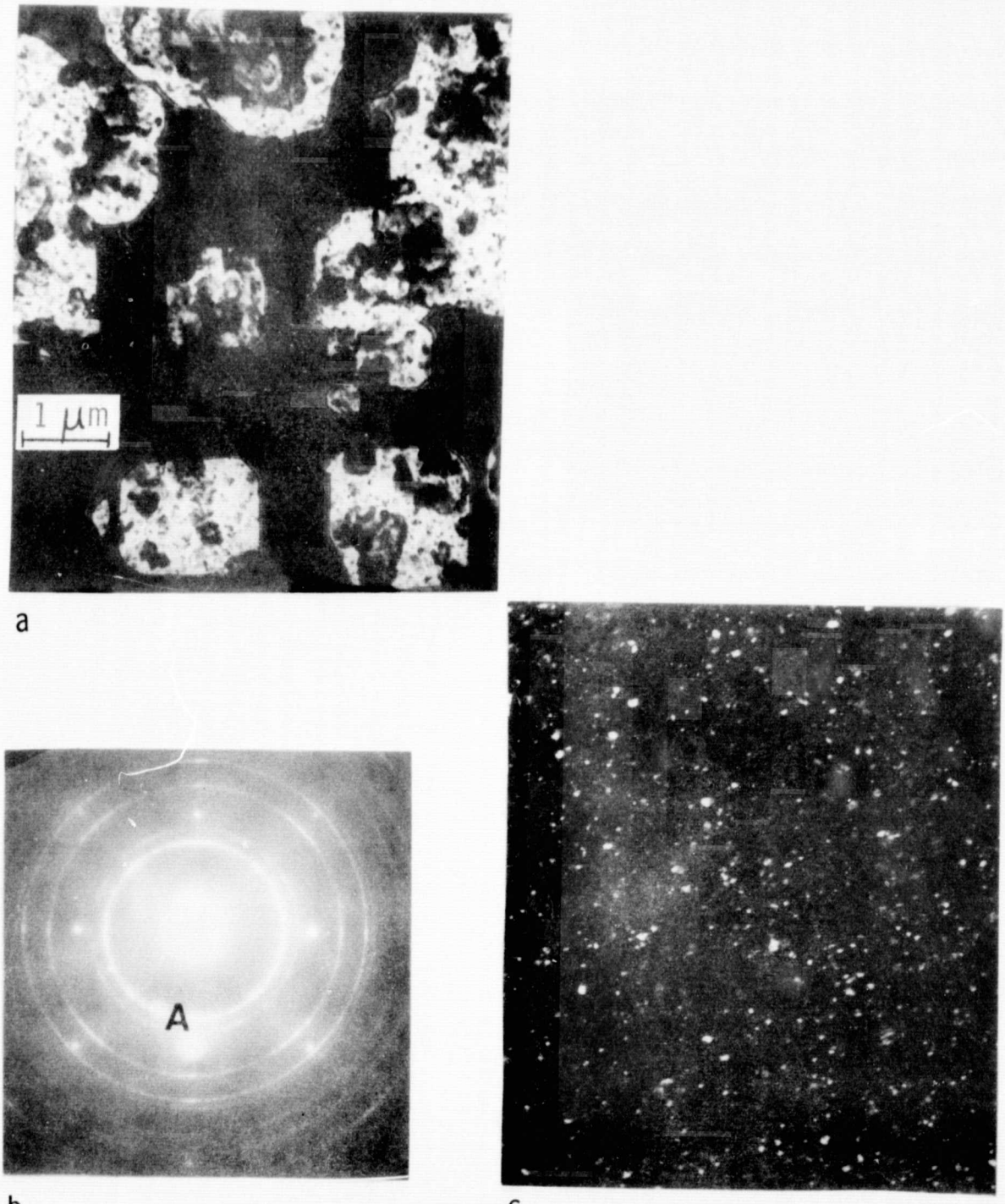

Fig. 2. TEM micrographs showing (a) β-SiC film on (001) seed surface, (b) electron diffraction pattern of (a), and (c) dark-field image taken from A in (b).

TABLE I. Identification of Surface Film on Crystal Seed

Surface Film d, Å	Reflection HKL	ASTM #1-119, β-SiC d, Å
2.510	111	2.51
2.173	200	2.17
1.541	220	1.54
1.298	311	1.31
1.258	222	1.26
1.089	400	1.09
0.999	331	1.00
0.972	420	0.97
0.888	422	0.89
0.837	333, 511	0.84
0.767	440	0.77
0.733	531	0.74

Similar transmission electron micrographs of specimens taken from the ribbon at positions close to the interface indicate that the surface film on the ribbon also consists of SiC crystals. However, the crystallite size is approximately 1 μm. Examples of such crystallites are given in Figs. 3a-c. Figure 3a is a standard bright-field micrograph, while Fig. 3b is the corresponding dark-field picture obtained by placing the "limited" aperture at a section of the (111) SiC ring (Fig. 3c). This result

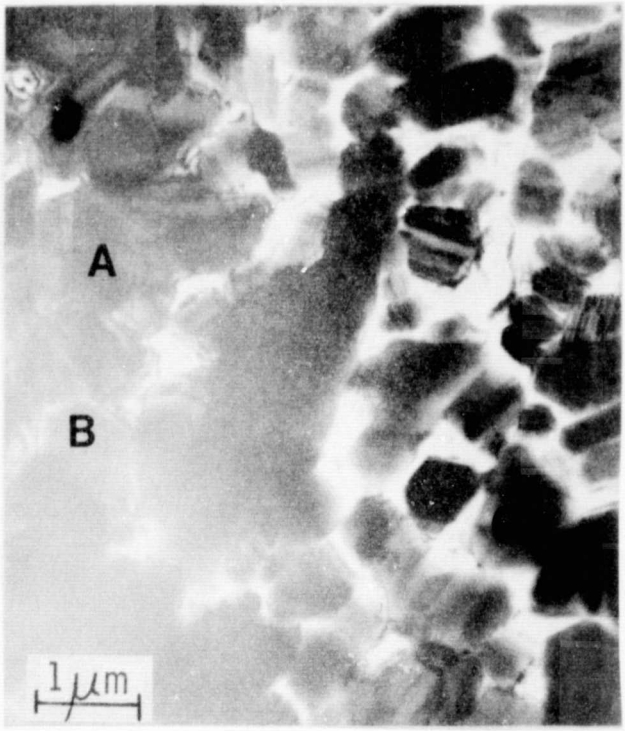

a

b

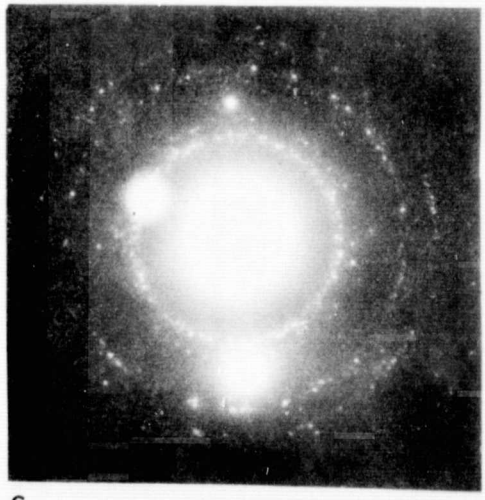

c

Fig. 3. TEM micrographs showing (a) the bright-field image, (b) the dark-field image of β -SiC particles on ribbon surface close to seed-ribbon interface, (c) corresponding electron diffraction pattern.

identifies the grains marked A, B, and C in Fig. 3a as β-SiC. Moving the aperture around the (111) SiC ring to different positions causes crystallites of different orientation to show up successively in the corresponding micrographs. From such observations it follows that the film consists of randomly oriented β-SiC crystals.

Interesting and instructive results are obtained through the transmission electron microscopy analysis of the dendritic structures. Dendritic structures on ribbon surfaces have been found for growth rates of 12 mm/min to 30 mm/min. The dendrites occur randomly over the ribbon surface or preferentially along grain boundaries, and are of submicron size for faster growth rates. Consequently, they may not yield to optical inspection. The dendrites have been found to influence generation lifetime of the silicon ribbon surfaces. A detailed investigation of their influence on generation lifetime in silicon ribbons is in progress.

The transmission electron micrographs of a dendritic cluster in bright and dark fields are shown in Figs. 4a and b. The corresponding transmission electron diffraction pattern is presented in Fig. 5a; the diffraction pattern is reproduced schematically in Fig. 5b. The diffraction pattern of Fig. 5a contains the basic [001] silicon diffraction pattern, but, in addition, every silicon reflex is surrounded by characteristic satellite reflexes.

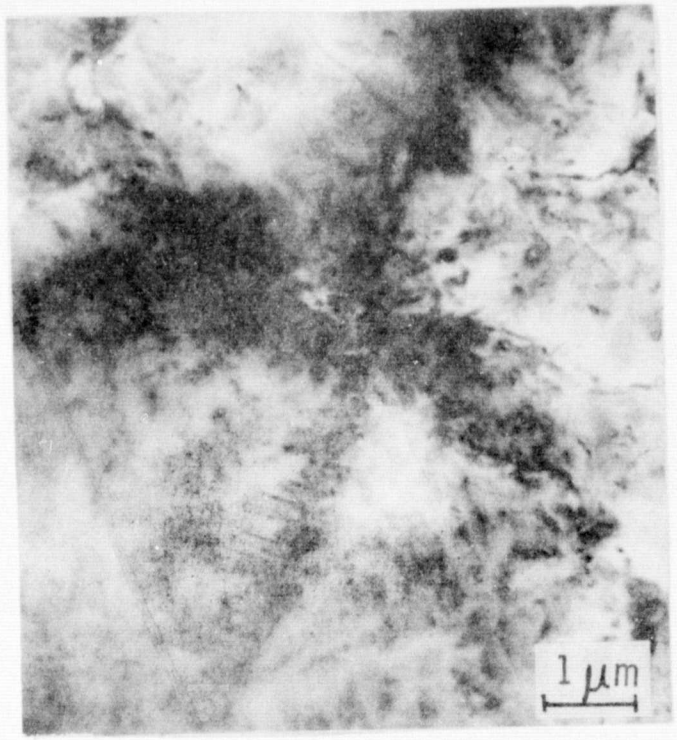

a

b

Fig. 4. TEM micrographs showing (a) bright-field image and (b) dark-field image of a dendrite cluster.

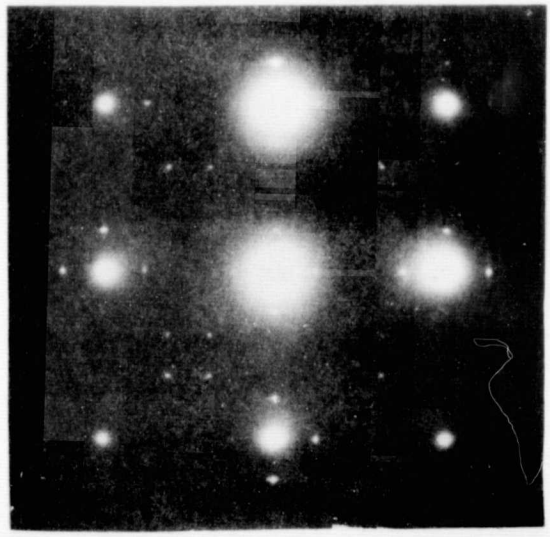

a

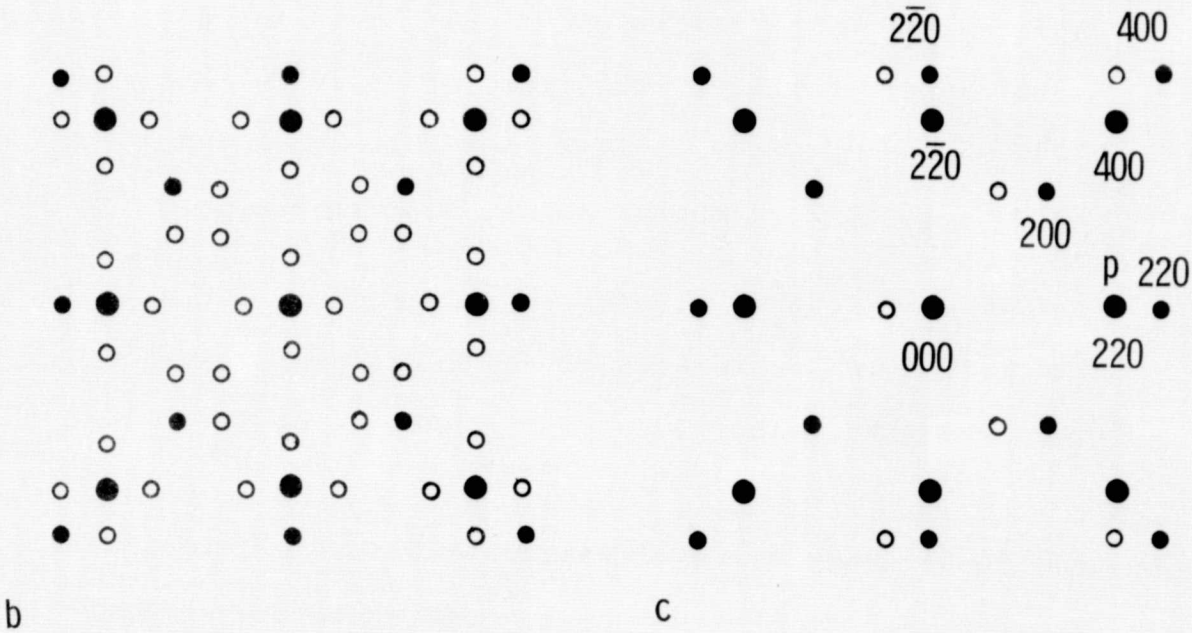

b c

Fig. 5. (a) Selected-area electron diffraction pattern of Fig. 4, (b) schematic drawing of (a), (c) superposition of β-SiC and Si (001) diffraction patterns with Si (220) reflex p acting as a secondary source for double diffraction. Large and small solid dots represent Si and β-SiC reflections, respectively. The small solid dots represent the double-diffraction spots due to p.

For analysis of the result contained in Fig. 5a the diffraction pattern of Fig. 5b was reconstructed with the following assumptions:

1. The dendrites consist of β-SiC and grow epitaxially with [001] orientation on the [001] oriented silicon. The epitaxial relationship between SiC and silicon is perfect for the (110) β-SiC planes parallel to the (110) silicon planes. Under such conditions, extra diffraction spots due to SiC appear in the silicon pattern. The distance between the silicon main reflex and any (h,k,l) diffraction spot due to β-SiC is obtained as follows. The ratio of lattice constants between β-SiC (a = 4.358 Å) and silicon (a = 5.403 Å) is 0.803. In reciprocal space, this corresponds to a distance of 1:0.803 = 1.245. Consequently, any (h,k,l) SiC reflection is located at the distance 1.245 <h,k,l> from the main beam.

2. Additional satellite reflexes around the silicon dots are produced by the epitaxial β-SiC phase due to double reflection. Double diffraction occurs if a diffracted beam from the silicon passes into the epitaxial SiC, or vice versa. In both cases the double-diffracted beam is determined by adding together the reciprocal lattice

vectors corresponding to the two component diffractions. Extra reciprocal lattice points displaced from the silicon matrix result.

Taking these two mechanisms into consideration and the additional fact that double diffraction from SiC (400) planes is found to be very weak, the diffraction pattern of Fig. 5c was constructed. The large solid spots in this pattern are due to silicon of <001> orientation. The small solid dots represent the SiC reflections, and the open-small dots represent the double-diffraction spots for the silicon reflex (220), p, acting as a secondary source. If this pattern is reproduced for the four (220) and four (400) silicon reflexes acting as secondary sources and the results are superimposed into a single schematic pattern, the superposition yields the pattern given in Fig. 5b, which describes exactly the diffraction pattern of Fig. 5a.

Additional information on the epitaxial relationship between β-SiC and Si is obtained through tilting experiments in the electron microscope. Analysis of electron diffraction patterns of [114], [112], and [$\bar{1}$14] orientation yields the orientation relationships summarized in Table II.

TABLE II. Epitaxial Relationship Between β-SiC and Si

Orientation	Orientation Relationship β-SiC parallel	Si
114	$[31\bar{1}]$	$[31\bar{1}]$
	$[13\bar{1}]$	$[13\bar{1}]$
112	$[3\bar{1}\bar{1}]$	$[3\bar{1}\bar{1}]$
	$[11\bar{1}]$	$[11\bar{1}]$
$\bar{1}14$	$[3\bar{1}1]$	$[3\bar{1}1]$
	$[1\bar{3}1]$	$[1\bar{3}1]$

Further insight into the SiC growth on silicon is obtained from the following results. Figure 6a shows the bright-field micrograph of a dendrite on a <112> ribbon surface. This particular surface plane is perpendicular to (111) crystal planes. This surface orientation is the result of twinning as described in the third quarterly report (2). The dendrite grows again preferentially in $\langle 1\bar{1}0\rangle$ directions. This is similar to dendrites growing on <001> ribbon surfaces. Interesting is the dark-field image of this dendrite recorded through use of the $(2\bar{2}0)$ β-SiC reflection, as indicated in Fig. 6c. The dark-field image is given in Fig. 6b and shows a group of parallel layers spaced at approximately 500 Å in the $[1\bar{1}0]$ direction. This result indicates that the dendrites consist of a succession of silicon and SiC layers which are stacked along (111) planes.

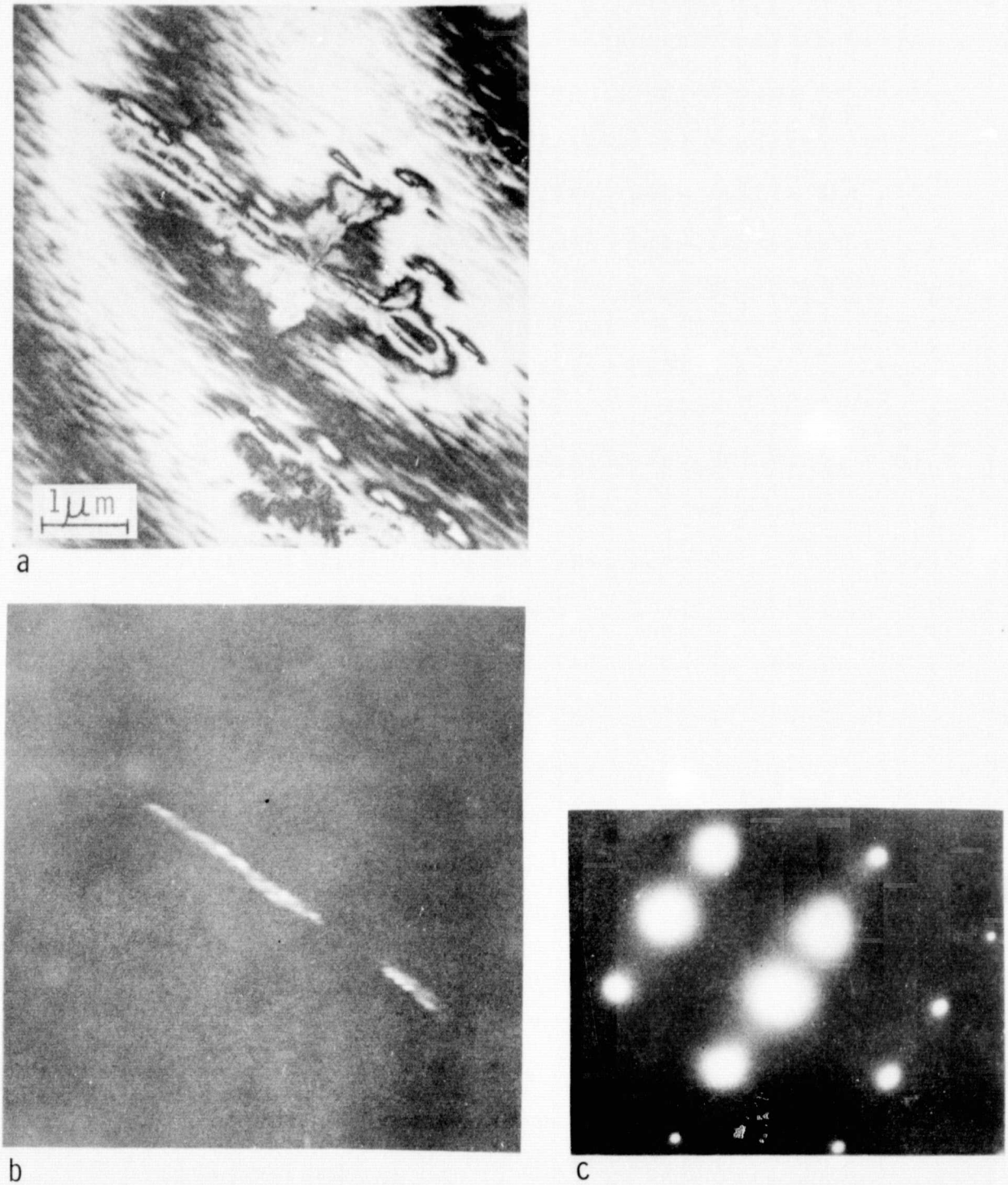

Fig. 6. TEM micrographs showing (a) bright-field image, (b) dark-field image of a dendrite on a <112> ribbon surface, and (c) electron diffraction of (a) and (b).

The electron diffraction pattern of Fig. 6c indicates that the epitaxial relationship between β-SiC and silicon is (112) β-SiC parallel to (112)Si, with $(2\bar{2}0)$ β-SiC parallel to $(2\bar{2}0)$, and $(11\bar{1})$ β-SiC parallel to $(11\bar{1})$Si. Fig. 6c is essentially identical with the diffraction pattern taken by tilting a [001]-oriented specimen into the [112] orientation.

The simple epitaxial relationship observed in this study is in good agreement with the results reported previously (3-5). Brown and Watts (3) and Jacobson (4) reported that the growth of β-SiC on (001) silicon substrates, by use of chemical vapor deposition, results in the orientation relationship of (001) β-SiC parallel to $(00\bar{1})$Si with (220) β-SiC parallel to (220)Si, and $(2\bar{2}0)$ β-SiC parallel to $(2\bar{2}0)$ Si. On (110) and (111) silicon substrates, similar epitaxial relationships are established between β-SiC and the silicon substrate (3,5).

5. SUMMARY

Surface films on silicon ribbons grown by the capillary action shaping technique by use of carbon dies are analyzed through optical and transmission electron microscopy. The films are formed through vapor deposition and consist of β-SiC. The SiC shows significant structural differences,

depending on deposition location - seed or ribbon - and on ribbon growth speed. On the seed surface the SiC deposits as randomly oriented crystallites ranging in size from 700 to 1500 Å. Close to the seed-ribbon interface the crystallite size increases to 1 μm. The small crystals are of well-defined crystallographic shape. With the increasing speed of silicon ribbon growth, epitaxial formation of SiC dendrites on the silicon ribbon surface becomes the dominant SiC growth mechanism. The epitaxial growth of β-SiC occurs through preferential incorporation of (111)SiC planes parallel to (111) silicon planes according to the epitaxial relationship (001) β-SiC parallel to (001)Si with (110) β-SiC parallel to (110)Si, and $(1\bar{1}0)$ β-SiC parallel to $(1\bar{1}0)$Si.

6. REFERENCES

1. Quarterly Technical Progress Report Number 1, JPL Contract 954144, G. H. Schwuttke, Principal Investigator, August 1975.

2. Quarterly Technical Progress Report Number 3, JPL Contract 954144, G. H. Schwuttke, Principal Investigator, March 15, 1976.

3. A. S. Brown and B. E. Watts, J. Appl. Crystallogr. 3, 1972 (1970).

4. K. A. Jacobson, J. Electrochem. Soc., 118, 1001 (1971).

5. I. H. Khan, Mater. Res. Bull. 4, S285, Pergamon Press, Inc. (1969).

CURRENT OUTLOOK FOR LARGE-AREA SILICON SHEET - A TECHNOLOGY PROJECTION

by

A. Kran

1. INTRODUCTION

Interactive computer simulation is used to support the development of technological and economic data required to define the potential of silicon-sheet growth for large-scale photovoltaic applications. The silicon-ribbon growth production-unit model simulates the complex interactions between physical variables pertaining to ribbon processing and the economic parameters associated with product manufacturing and business management.

As described in the second quarterly report (1), the production-unit concept, together with technology forecasting and sensitivity analysis, was used to compare single- and multiple-ribbon growth systems for their ability to provide low-cost silicon-sheet material. Conclusions favored single-ribbon growth and suggested that processing-technology improvements offered the best potential for achieving low-cost silicon-sheet material objectives within the shortest period of time. This report

extends that work to include an assessment of energy-capacity cost at the sheet material level, using system simulation and probability concepts (2). It also associates technology parameters projected in time with an estimated probability of the event's occurring at a specific point. This results in a cost ($/kWE) versus time relationship and in an ability to compare our projections of future sheet material cost with ERDA projections for solar-array costs.

Since single-ribbon growth, on the basis of previous work, appeared to have more potential for achieving low-cost material objectives, no further analysis of multi-ribbon growth is planned without additional data.

2. TECHNOLOGY FORECASTING METHODOLOGY

2.1 General

Technology forecasting, today, is recognized as an integral part of the decision-making process, leading to a commitment of resources to future products. Properly structured and applied, it is a useful tool for looking ahead to increasingly complex technology and to an environment marked by rapid changes. Technology forecasting is also a

structure for communication, requiring the forecaster to define his terms and open to challenge his technical expertise, data, thought process, and biases. It compels him to make his assumptions explicit, which does not guarantee the correctness of forecast, but does offer the opportunity to confirm assumptions and to ensure that the data used are the best available.

Many forecasting techniques are reported in the literature. Most concern themselves with the evolution of a product, such as a computing system, calculator, or automobile, and involve the fitting of some mathematical function or curve to historical data. The forecast is obtained by projecting the fitted curve into the future. Learning-curve analysis is an example of this type of general, aggregate projection, which is useful for reviewing the general viability of a product or technology. Once a project is under way, however, more specific monitoring and projection techniques must be added, so that progress from a "bottoms-up" point of view can be compared with management-stated "tops-down" program objectives.

2.2 Forecasting Technique

Our procedure for forecasting silicon-sheet manufacturing technology is predicated upon the production-unit concept:

1. Define a specific production unit.

2. Project technology capability of parameters.

3. Introduce chronology.

4. Evaluate numerically to obtain cost vs time.

The production-unit approach reduces the complexity of interaction among processing sectors in a manufacturing operation, and may be thought of in terms of three elements: processing technology, resources, and raw materials. Its purpose is to transform polycrystalline bulk silicon into sheets of single-crystal or controlled-crystallography material suitable for solar-cell fabrication. These three elements are described to the system as a specific combination of manpower, crystal-growing equipment, and polycrystalline silicon needed to progress through the crystal-pulling sector in a solar-cell manufacturing operation.

The "baseline" production unit, or starting point for the projection, is developed from specific data which reflect processing technology practiced in the laboratory and assumed transferable to a production environment, and from estimated direct- and indirect-cost items, plus profit, representative of a small- to medium-size concern. From this baseline, any one of the 27 model parameters can be projected in terms of what is anticipated in the "near-future" (soon), what is expected in the "future," and what will be approached as the "limit." This is done without commitment to a specific time frame. Subsequently, in order to introduce chronology, these technology projections are associated with a probability of meeting particular technology objectives by a specific point in time. For example (as further discussed in section 2.4), we estimate for 1985, with a probability of 70%, that ribbons between 10 and 25 cm wide will be routinely pulled. After numerical evaluation of the cumulative probability distribution function, calculation of energy cost at the level of silicon-sheet material, and statistical analysis of these cost figures, a cost-versus-time curve is plotted.

This forecasting technique requires two projections: the first, relating to technology and its limits, should be

provided by the technologist; the second, pertaining to the probability of implementing stated technology objectives, is more management-oriented, as implementation schedules depend upon allocation of resources to develop the technology. Finally, because this technique is readily applied and rapidly iterated, it lends itself well as a tool to be used jointly by technology developers and planners interested in tracking development progress and cost profiles.

2.3 Baseline Definition

The baseline production unit may be thought of as a reference point from which all projections are made. The list of 27 input parameters to the model is shown in Fig. 1 and is divided into three categories. The ribbon data category contains processing-related parameters, such as ribbon width (2.5 cm), growth rate (1.5 m/hr), and thickness (0.3 mm). Wherever possible, such as in the case of ribbon width, growth rate, or thickness, state-of-the-art values are used.

The direct-cost category comprises the crystal-growth system cost - which, at $50,000, is essentially the cost of a Czochralski puller modified for ribbon growth - equipment life (7 years), and interest rate (10%), so that equipment

```
  RIBBON DATA FROM SIMULATIONS 37 38 39 DATED 11/04/75
1  RIBBONS GROWN SIMULTANEOUSLY -      1    1    1
2  RIBBON WIDTH, CM -          2.5  2.5  2.5
3  RIBBON GROWTH RATE,M/HR -    1.50  1.50  1.50 ..OR AS PCT  30  30  30
4  RIBBON THICKNESS, MM -  0.30 0.30 0.30
5  YIELD OF CELL QUALITY RIBBON, PCT -    70  75  80

  DIRECT COST
6  RIBBON FURNACE, DOLLARS -    50000  50000  50000
7     EQUIPMENT LIFE, YEARS -    7.0  7.0  7.0
8     INTEREST RATE, PERCENT -   10.0 10.0 10.0
9     EQUIPMENT AVAILABILITY, PERCENT -     70   75   80
  PERSONNEL PER SHIFT PER MACHINE
10 11 NO. OF SUPVS -   0.05 0.05 0.05 AT $ -  25000 25000 25000
12 13 NO. OF ENGRS -   0.10 0.10 0.10 AT $ -  20000 20000 20000
14 15 NO. OF TECHN -   0.50 0.50 0.50 AT $ -  10000 10000 10000
16 POLY SILICON COST, DOLS/KG -    65  65  65
17 POLY YIELD TO RIBBON,PERCENT -    80  83  85
  SERVICES AND SUPPLIES
18    CRUCIBLE/DIE/PARTS COST PER DAY -    30  30  30 DOLLARS
19    POWER COST AT -  0.05 0.05 0.05 DOLLARS PER KWH
20    ENERGY TO OPERATE EQUIPMENT -    12  12  12 KW

21 22  O/H -   50  50  50 PCT OF PERS+   10  10  10 PCT OF RAW MATL COST
23  G_AND_A -   10  10  10 PERCENT OF DIRECT COST+OVERHEAD

24  PROFIT BEFORE TAX, PERCENT - 10 10 10 OF DC+O/H+G&A

  MISCELLANEOUS
25 WORKWEEK, HOURS -  168 168 168
26 CONVERSION EFFICIENCY, PERCENT -    8.00  8.00  8.00
27 ENERGY DENSITY AT AM1,KW/SQ M PEAK -     1    1    1
```

Fig. 1. Baseline input parameters to production unit.

capital recovery can be calculated. Equipment availability is defined as the percent of time the system is available for crystal pulling, excluding setup, polysilicon melt-down, and random machine failure time. Also included here are the direct personnel required to assure efficient operation of the system, polysilicon cost, and services and supplies, which include die cost. Overhead, general and administrative expenses, and profit are defined as percentages relating to other direct-cost items.

The third category defines the workweek in terms of hours and of energy-conversion efficiency at AM1, a hypothetical value to assess energy-capacity cost at the level of silicon-sheet material.

Since ribbon growth is still considered to be in the development, not manufacturing, phase, parameters such as yield of "cell quality" (suitable for solar-cell fabrication) ribbon, poly yield to ribbon, and machine availability are estimated in terms of what could be expected in a production environment on the basis of laboratory experience. Since these values are subject to interpretation, three cases are shown, reflecting an outlook ranging from conservative to optimistic.

Output from the model, shown in Table I, consists of the major factors contributing to sheet material and energy-capacity cost. For our purposes, the most conservative values (energy-capacity cost: $8476/kWE peak) are used as the baseline. They include the average yielded growth rate (0.02 m^2/hr), the yield factor (0.56), plus the following direct-cost elements, calculated in dollars/m^2: equipment capital recovery, personnel, polysilicon, and services and supplies. Also calculated in dollars/m^2 are overhead cost, G&A expense, and profit. The addition of these items results in a total dollars/m^2 figure for silicon-sheet material ($678), representing a selling price to a manufacturer, or purchase cost to a buyer.

TABLE I. Economics of Silicon Ribbon (Baseline) — One Ribbon Puller

SIMULATION ID AND NO.: 11/04/75	37	38	39
RIBBONS GROWN SIMULTANEOUSLY	1.00	1.00	1.00
RIBBON WIDTH, CM	2.50	2.50	2.50
AVG YIELDED GROWTH RTE,SQ M/HR	0.02	0.02	0.02
COMBINED YIELD FACTOR	0.56	0.62	0.68
DIRECT COST IN DOLS/SQ METER			
EQUIPMENT CAPITAL RECOVERY	66.54	57.96	50.94
PERSONNEL	224.49	195.56	171.88
POLY SILICON COST	81.13	72.99	66.82
SERVICES/SUPPLIES	71.45	63.66	57.20
SUBTOTAL:	443.61	390.17	346.84
OVERHEAD COST IN DOLS/SQ METER	116.79	102.32	90.48
G&A EXPENSES IN DOLS/SQ METER	56.04	49.25	43.73
PROFIT IN DOLLARS/SQ METER	61.64	54.17	48.11
TOTAL COST IN DOLS/SQ METER	678.08	595.91	529.16
DOLLARS PER KW	8476.03	7448.89	6614.44

2.4 Parameter Projection and Numerical Evaluation

All technology projections are made from the baseline and address three future points in time: near-future, future, and limit. These points define the expected capabilities of the particular technology, silicon-sheet growth in this case, from its state-of-the-art to full maturity. Chronology is introduced by estimating the probability of meeting the objective associated with the technology parameter at a stated point in time.

Ribbon-width capability is used to illustrate this technique. As can be seen from Table II, we project for 1980, with a probability of only 0.05, that ribbons between 2.5 cm wide, our current baseline, and 5 cm wide will be

TABLE II. Ribbon-Width Capability

	Present		Near-Future		Future		Limit
Width (cm)	2.5	↑	5	↑	10	↑	25
Probability							
1980:		.05		.65		.30	=1.0
1985:		.02		.28		.70	=1.0

routinely pulled. In other words, we are convinced that this capability will be achieved. We estimate the same probability to be 0.65 that ribbon width will be between 5 and 10 cm, and 0.30 that ribbon width will be between 10 and 25 cm. The probabilities are mutually exclusive and add up to 1. For 1985, the probabilities are 0.02, 0.28, and 0.70, respectively. A graphical representation of the foregoing is shown in Figs. 2 and 3.

The probability is continuous and even for each point between the three intervals, as is seen from the 1980 cumulative distribution function shown in Fig. 4, where we transform a uniformly distributed sequence of random numbers (y-axis) into one that is non-uniformly distributed and that is based upon our estimated probability distribution (x-axis). This cumulative probability distribution function is then evaluated numerically, as seen in Figs. 5 and 6. For example, using the same random number (0.55), Fig. 5 (1980) yields a 9-cm-wide ribbon, whereas Fig. 6 (1985) yields a 15.5-cm-wide ribbon.

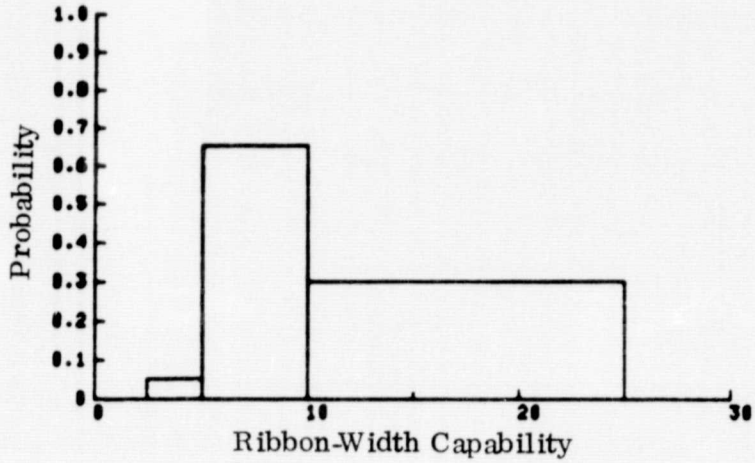

Fig. 2. Ribbon-width capability vs 1980 probability.

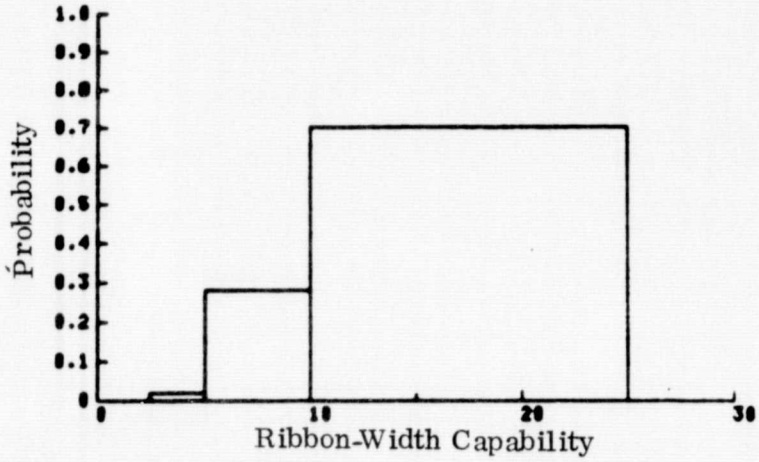

Fig. 3. Ribbon-width capability vs 1985 probability.

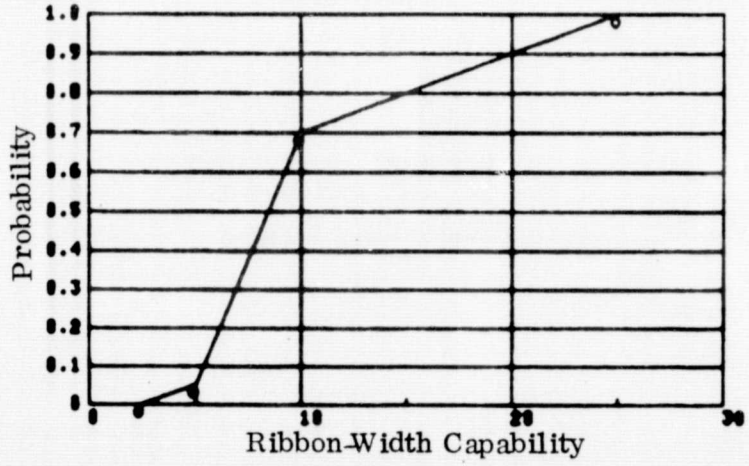

Fig. 4. Ribbon-width capability vs 1980 cumulative probability.

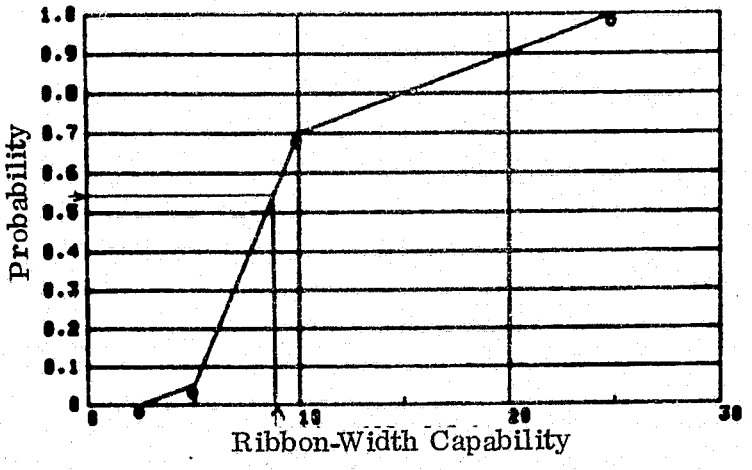

Fig. 5. Ribbon-width capability vs 1980 cumulative probability--example of numerical evaluation technique.

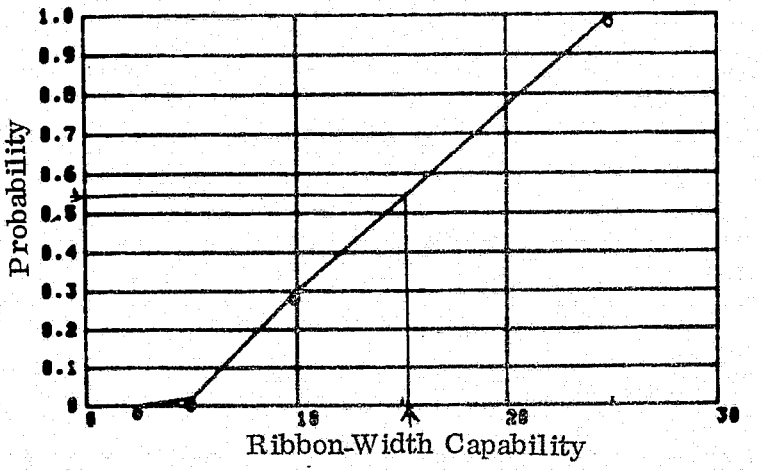

Fig. 6. Ribbon-width capability vs 1985 cumulative probability--example of numerical evaluation technique.

3. COMPUTER PROGRAM FOR TECHNOLOGY FORECASTING

3.1 Data Flow Model

The computer program is written in APL, a high-level programming language, and provides an interactive system for technology projection. Its operation is briefly described in conjunction with the data flow model shown in Fig. 7.

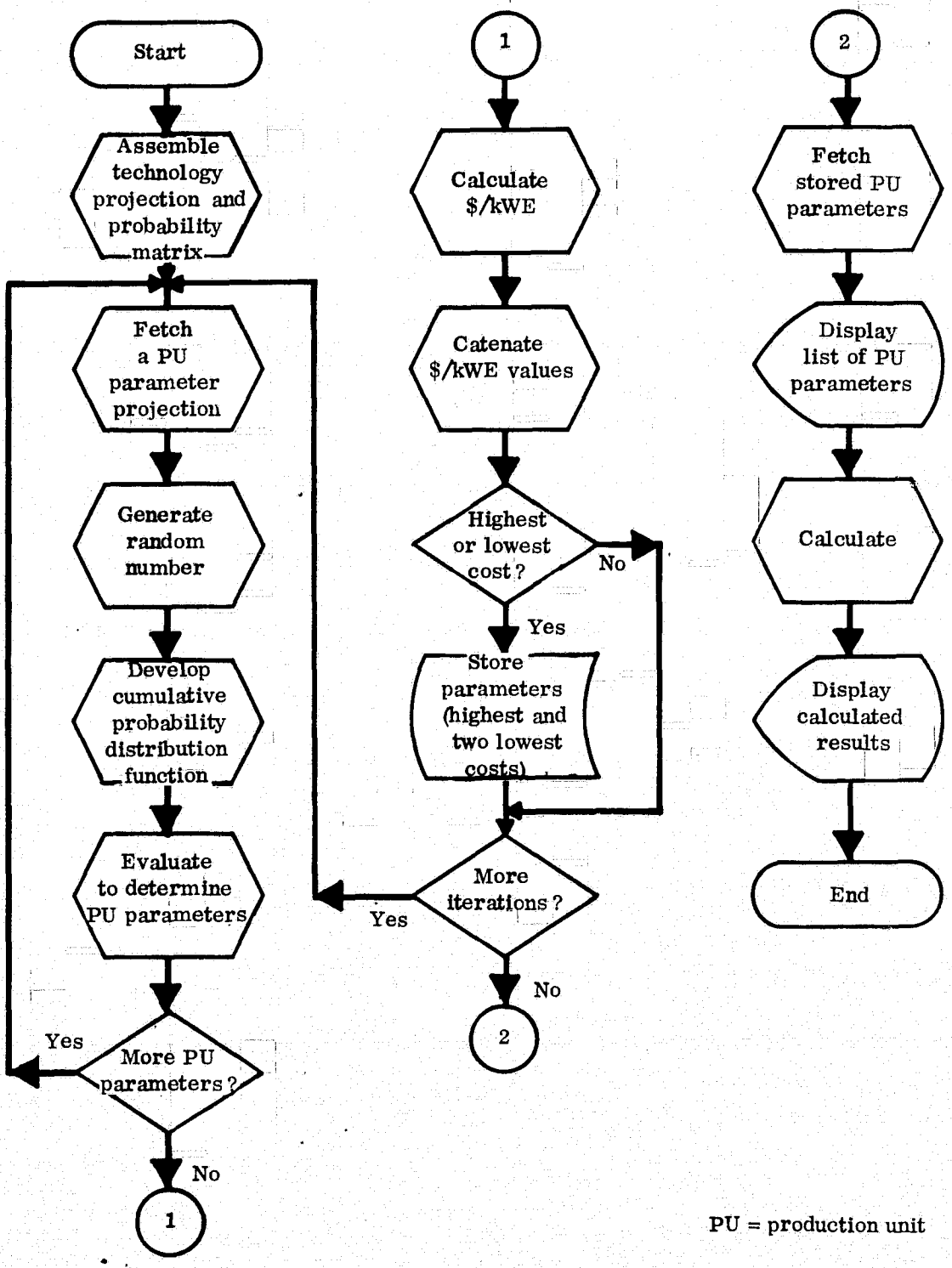

Fig. 7. Technology-forecasting data flow model.

The program operates on a 27-by-8 matrix, containing 4 columns of production-unit values and 3 columns of estimated probabilities pertaining to them (see section 4.2). As depicted in Fig. 7, the program fetches the first row of the matrix, generates a random number, develops the appropriate cumulative distribution function from the given probabilities, and then numerically evaluates the cumulative distribution function, using a random number generator, to determine the specific production-unit parameter. It then proceeds to the next row until a complete set (27) has been developed. Subsequently, energy-capacity costs (three) at the silicon-sheet material level are calculated (Fig. 1) and stored, as are three sets of input parameters (those resulting in the highest and two lowest $/kWE figures). This operation is iterated the number of times specified (600 cost figures each for 1980 and 1985). Finally, a statistical analysis provides the data points for the curve (shown in section 4.5).

3.2 Listing of Functions

Following is a display of functions needed to operate the program in conjunction with the code published in Ref. 1. The computer code is documented to facilitate understanding and maintenance by others.

```
DESCRIBE

THESE  FUNCTIONS  IN CONJUNCTION WITH  THE  PRODUCTION  UNIT
MODEL   CONSTITUTE  AN  INTERACTIVE  SYSTEM  FOR  TECHNOLOGY
PROJECTION OF ENERGY CAPACITY COST  AT  THE LEVEL OF SILICON
SHEET MATERIAL (DOLS/KWE).

     THE _SYSTEM_ CONTAINS THREE _USER _ACCESSED  FUNCTIONS,
"DEFINE ,"MODIFY",  AND   PROJECT .    DEFINE  SETS UP THE
GLOBAL  MATRIX  PR,  WHICH  MAY  BE  CHANGED  BY     MODIFY .
 PROJECT   OPERATES ON PR,  CALCULATING ENERGY CAPACITY COST
AND KEEPING THREE SETS OF  INPUT  VARIABLES -THOSE RESULTING
IN THE HIGHEST AND TWO LOWEST ENERGY CAPACITY COSTS.   ABOUT
2500 PROJECTIONS CAN BE CALCULATED, BEFORE THE  WORKSPACE IS
FULL.



      ∇DEFINE[□]∇
    ∇ DEFINE;A;B;C;K
[1]   ⍝⍝   COMPILES GLOBAL MATRIX PR. 27 ROWS×4PROJ+3EST
[2]   ⍝⍝   ALSO A SAMPLE GU MATRIX FOR PU MODEL
[3]    ' USE EITHER FORMAT FOR ENTRY:'
[4]    '   2 5 10 25 .3 .4 .3 (7 ENTRIES)'
[5]    '   5 10 25 (THEN VECTOR IS X[1 5 6 7]←0 1 1 1'
[6]    '   2 5 10 25 3 4 3 (X[5 6 7] IS DIV BY 10)'
[7]    A← 27 3 ⍴0
[8]    B← 27 7 ⍴0
[9]    K←0
[10] LOOP:
[11]   →(27<K←K+1)↑END
[12]   'ENTER ROW ',⍕K
[13]   →(7=⍴C←,□)↑G0
[14]   C←0,C,3⍴1
[15] G0:
[16]   →((+/C[5 6 7])≠10)↑G1
[17]   C[5 6 7]←C[5 6 7]÷10
[18] G1:
[19]   ⍝    ROWS:7 MEMBER VECT,+/~3↑C<=1 OR 3
[20]   ⍝
[21]   →((7=⍴C)∧((1=+/~3↑C)∨(3=+/~3↑C)))↑G2
[22]   'ROW ',(⍕K),' INPUT NOT ACCEPTABLE ',⍕C
[23]   K←K-1
[24]   →LOOP
[25] G2:
[26]   A[K;]←PP⍵,B[K;]←C
[27]   GU←A
[28]   PR←B
[29]   →LOOP
[30] END:
     ∇


      ∇MODIFY[□]∇
    ∇ MODIFY X;A;K
[1]   ⍝⍝   MODIFIES GLOBAL MATRIX PR
[2]   ⍝      RIGHT ARGUMENT<=ROW NUMBER(S)
[3]    'USE FORMAT: 2 5 7 10 .5 .3 .2'
[4]    X←,X
[5]    K←0
[6]   LOOP:
[7]    →((⍴,X)<K←K+1)↑END
[8]    'ENTER ROW ',⍕(X[K])
[9]    A←,□
[10] ⍝    INPUT MUST BE 7 NUMBS,+ ~3↑A<=1 OR 3
[11]  ⍝
[12]   →((7=⍴A)∧((1=+/~3↑A)∨(3=+/ ~3↑A)))/G0
[13]   'ROW ',(⍕X),' INPUT NOT ACCEPTABLE: ',⍕A
[14]   K←K-1
[15]   →LOOP
[16] G0:
[17]   PR[X[K];]←A
[18]   →LOOP
[19] END:
     ∇
```

```
▼PROJECT[0]▼
    ▼ PROJECT X;A;B;D;K
[1]   ⍝⍝     CALCS PROJCTD ENERGY CAPACITY COSTS (DOLS/KWE)
[2]   ⍝⍝     FROM GV LIST PROVIDED BY RNL. INPUT TO STAT WS
[3]   ⍝       RIGHT ARGUMENT←→NO OF SETS(3)TO BE EVALUATED
[4]   ⍝       RESULT IS 3×X EN (COSTS) PLUS DISPLAY OF
[5]   ⍝       THREE (HIGHEST,2LOWEST) PRODUCTION UNITS
[6]    DRL←1000000
[7]    EN←⍳B←K←0
[8]    D←1000000
[9]    A← 27 3 ⍴0
[10]  G1:
[11]   →(X<K←K+1)↑PRT
[12]   RNL 1
[13]   GV[3;]←UNP GV[3;]
[14]   CONVERT
[15]   CALC
[16]   EN←⌈EN,⍤NC
[17]   →(K≠1)↑H0
[18]  ⍝
[19]  ⍝   PICK MID-VALU GV COLUMN TO INITIAL [37]
[20]  ⍝
[21]   A[;3]←GV[;1↑1+⍤NC]
[22]  H0:
[23]  ⍝
[24]  ⍝   B←→ HIGHEST EN VALUE
[25]  ⍝
[26]   →(B≥(⌈/⍤NC))↑G2
[27]  ⍝
[28]  ⍝   RETAIN COLUMN OF GV RESULTING IN HIGHEST EN
[29]  ⍝
[30]   A[;1]←GV[;⍤NC↑⌈/⍤NC]
[31]   B←⌈/⍤NC
[32]  G2:
[33]   →(D≥(⌊/⍤NC))↑G1
[34]  ⍝
[35]  ⍝   RETAIN GV COLMS RES IN 2 LOWEST EN VALUES
[36]  ⍝
[37]   A[;2]←A[;3]
[38]   A[;3]←GV[;⍤NC↑⌊/⍤NC]
[39]   D←⌊/⍤NC
[40]   →G1
[41]  PRT:
[42]   GV←A
[43]   CONVERT
[44]   LIST
[45]   B
[46]   CALC
[47]   DISPLAY1
    ▼


▼PPR[0]▼
    ▼ Z←PPR X;A;B;K
[1]   ⍝⍝    CALCULATES 3 PRODUCTION UNIT PARAMETERS
[2]   ⍝⍝    FROM TECHN PROJECTION AND EST PROBABILITY,
[3]   ⍝⍝    USING RANDOM NUMBERS
[4]   ⍝      RIGHT ARGUMENT ←→ 4 TECH PROJ,3 EST PROB
[5]   ⍝      EXPLICIT RESULT ←→ 3 PROD UNIT PAR VALUES
[6]   ⍝
[7]   ⍝    IF +/⍤3↑X IS 3 AND X[1] IS NOT 0,
[8]   ⍝    TECHN LIMIT HAS BEEN REACHED.PROJ IS N/A
[9]   ⍝
[10]   →((3≠+/⍤3↑X)∨(0=1↑X))/H1
[11]   Z←3⍴X[1]
[12]   →0
[13]  H1:
[14]  ⍝    IF +/⍤3↑X IS 3, PARAMETER IS NOT BEING
[15]  ⍝    EVAL. X[1] SHOULD BE SET TO 0.
[16]  ⍝
[17]   →((⍳)/⍤3↑X)≠3)/H2
[18]   Z←X[2 3 4]
[19]   →0
[20]  H2:
[21]   →((+/X[5 6 7])=1)/H3
[22]   →0,⍞←'PROBABILITIES MUST=1'
[23]  H3:
[24]   Z←3⍴0
[25]  ⍝
[26]  ⍝    CALC SLOPE OF 3 LINE SEGMENTS.THIS IS CUM
[27]  ⍝    PROB DIST FN,X[1] AT Y←0,X[4] AT Y←1
[28]  ⍝
[29]   B←(X[2 3 4]-X[1 2 3])÷(+\X[5 6 7])-(+\(0,X[
      5 6]))
```

```
[30]  K←0
[31] LOOP:
[32] ⍝   EVAL CUM PROB DIST FN (3 VALUES)
[33] ⍝
[34]  →(3<K←K+1)/0
[35]  A←RAN
[36] ⍝
[37] ⍝     IS RANDOM NO IN 1ST LINE SEG RANGE?
[38] ⍝
[39]  →(A>X[5])/G1
[40] ⍝
[41] ⍝   PAR VAL IS X[1]+(B[1]×A)
[42] ⍝
[43]  Z[K]←X[1]+(B[1]×A)
[44]  →LOOP
[45] G1:
[46] ⍝
[47] ⍝   IS RAN NO IN 2ND LINE SEG RANGE?
[48] ⍝
[49]  →(A>+/X[5 6])/G2
[50]  Z[K]←(X[2])+(B[2]×(A-X[5]))
[51]  →LOOP
[52] G2:
[53] ⍝   IF RAN NO ≠ 1,IT MUST BE IN 3RD SEG
[54] ⍝
[55]  →(A≠1)/G3
[56]  Z[K]←X[4]
[57]  →LOOP
[58] G3:
[59]  Z[K]←(X[3])+(B[3]×(A-+/X[5 6]))
[60]  →LOOP
    ∇


      ∇RAN[□]∇
    ∇ Z←RAN
[1]  ⍝⍝   GENERATES A RANDOM NUMBER
[2]  ⍝⍝   BETWEEN .000001 AND 1
[3]  ⍝⍝   WITH EQUAL PROBABILITY
[4]  Z←(?1000000)÷1000000
    ∇


∇RNL[□]∇
    ∇ RNL X;A;B;D;K;K1
[1]  ⍝⍝   COMPILES PROD UNIT INPUT PAR VALUES GV
[2]  ⍝⍝   FROM GLOBAL MATRIX PR
[3]  ⍝     RIGHT ARGUMENT (⍵) NUMBER OF SETS
[4]  ⍝     ONE SET IS REQD AS INPUT TO FN CALC
[5]  ⍝
[6]  ⍝   D IS X BY 3 MATRIX TO INDEX GV
[7]  ⍝
[8]  D←(X,3)⍴⍳(X×3)
[9]  GV←(27,3×X)⍴0
[10] A← 27 3 ⍴0
[11] B←PR
[12] K1←K←0
[13] LOOP:
[14] ⍝   COMPILES A GV SET
[15] ⍝
[16] →(27<K←K+1)↑G0
[17] A[K;]←PPR B[K;]
[18] →LOOP
[19] G0:
[20] ⍝   GV SETS ARE LAMINATED
[21] ⍝
[22] →(X<K1←K1+1)↑END
[23] GV[;D[K1;]]←A
[24] K←1
[25] →LOOP
[26] END:
    ∇
      ∇UMP[□]∇
    ∇ Z←UMP X;A;T
[1]  ⍝⍝   CONVERTS RIBBON GROWTH RATE FROM ·/· TO ACTUAL
[2]  ⍝     RIGHT ARGUMENT (⍵) PERCENT
[3]  ⍝     EXPLICIT RESULT (⍺) ACTUAL GROWTH RATE
[4]  ⍝
[5]  ⍝   CONVERT THICKNESS TO MM
[6]  ⍝
[7]  T←GV[4;]÷10
[8]  ⍝
[9]  ⍝   CALCULATE UMAX FOR THICKNESS, THEN UMAX×X
[10] ⍝
[11]  Z←(÷100)×X×A←0.87911×((1÷T)*0.5)
    ∇
```

4. APPLICATION OF FORECASTING TECHNIQUE TO LARGE-AREA SILICON SHEET PROJECTION

4.1 Projection of Silicon Sheet Technology Parameters

The last quarterly report (3) concluded that single-ribbon growth and processing-technology improvement offered the best potential for achieving low-cost sheet-material objectives. Consequently, only technology-sensitive parameters (13 out of 27) are projected for this analysis, as shown in Table III. The first column contains the baseline, and the remaining three our projections.

TABLE III. Silicon Ribbon Technology Projection

Item No.	Parameter	Present	Near-Future	Future	Limit
2	Ribbon width (cm)	2.5	5	10	25
3	Ribbon growth rate (% of V_{max})	30	40	50	60
4	Ribbon thickness (mm)	0.30	0.20	0.15	0.10
5	Yield of "cell grade" ribbon (%)	70	80	90	95
6	Ribbon furnace cost ($\$ \times 10^3$)	50	25	20	15
7	Equipment life (years)	7	8	10	12
9	Equipment availability (%)	70	80	90	95
14	Number of technicians	0.50	0.25	0.15	0.10
16	Polysilicon cost ($/kg)	65	45	30	6
17	Poly yield to ribbon (%)	80	85	90	95
18	Services and supplies ($/day)	30	25	20	10
20	Energy to operate equipment (kWE)	12	11	10	3
26	Cell conversion efficiency (%)	8	10	12	15

Using the three projections as input to our production-unit model results in Table IV, where simulation numbers 43, 44, and 45 represent the "near-future," "future," and "limit" projections. Accordingly, we conclude at this point that silicon-sheet growth, as a technology, has the capability of providing the material at the required cost to meet a $500/kWE array-cost objective at a later point in time than represented by simulation number 44($314/kWE), but well before the technology limit is reached (simulation number 45, $42/kWE). This projection is plotted in Fig. 8 (lower curve), together with another one, independently arrived at. As can be seen, the difference between the two is insignificant.

TABLE IV. Near-Future, Future, and Limit Projection of Silicon Ribbon Technology

SIMULATION ID AND NO.: 11/04/75	43	44	45
RIBBONS GROWN SIMULTANEOUSLY	1.00	1.00	1.00
RIBBON WIDTH, CM	5.00	10.00	25.00
AVG YIELDED GROWTH RTE,SQ M/HR	0.08	0.29	1.19
COMBINED YIELD FACTOR	0.60	0.81	0.90
DIRECT COST IN DOLS/SQ METER			
EQUIPMENT CAPITAL RECOVERY	7.01	1.33	0.22
PERSONNEL	36.13	8.17	1.79
POLY SILICON COST	30.84	12.94	1.55
SERVICES/SUPPLIES	14.88	3.60	0.61
SUBTOTAL:	88.86	26.04	4.16
OVERHEAD COST IN DOLS/SQ METER	20.16	5.13	1.03
G&A EXPENSES IN DOLS/SQ METER	10.90	3.12	0.52
PROFIT IN DOLLARS/SQ METER	11.99	3.43	0.57
TOTAL COST IN DOLS/SQ METER	131.92	37.72	6.29
DOLLARS PER KW	1319.22	314.36	41.92

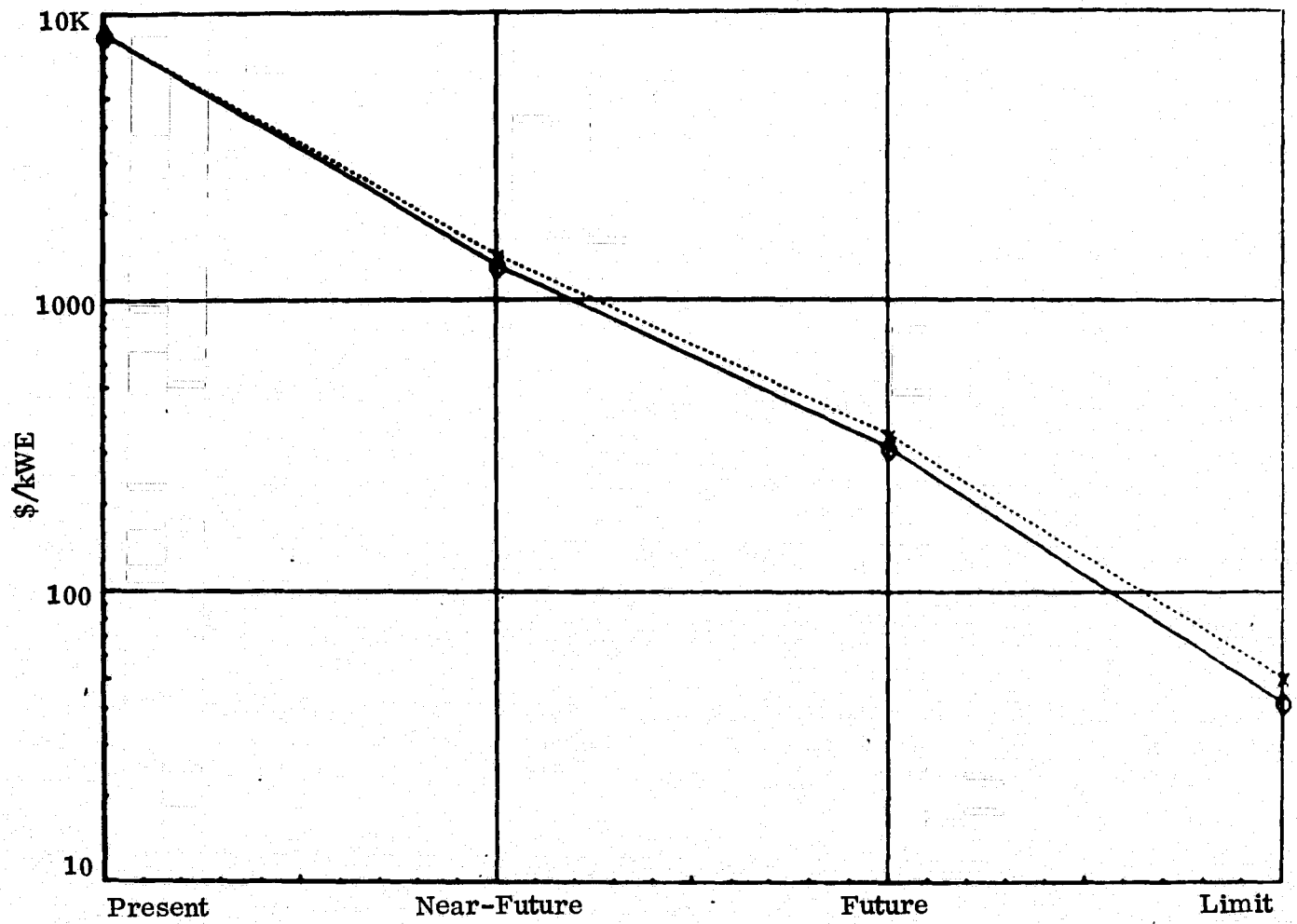

Fig. 8. Silicon ribbon technology projection.

4.2 Association Between Technology Capability and Time

As described in section 2.4, each technology parameter, in order to introduce chronology, is coupled to a point in time by means of an estimated probability that the projection will, in fact, materialize. Subsequently, the cumulative probability distribution function is evaluated numerically by computer, using a random number generator. The computer

program operates on a predefined 27-row by 8-column matrix. Although similar matrices could be developed for each year, only two were defined for this study (1980, 1985), shown as Tables V and VI. The first column of each matrix corresponds to the production-unit parameter item number (see Fig. 1). The next column represents the baseline, the following three are the projections, and the remaining three the estimated probabilities. Only the latter are changed to simulate the progression of time. For instance, the second row refers to ribbon width, with values previously shown in Table II. Whenever probabilities are listed as 1, the corresponding production-unit parameter is not subject to this probabilistic evaluation.

4.3 Approach to Parameter Projection

Application of this technique requires a technical understanding of what the technology is capable of achieving, an assessment of state-of-the-art, and, finally, judgment with respect to the timing of subsequent implementation. If silicon-sheet technology is to become cost-effective for photovoltaic applications, then improvement of width capability is of prime importance. During the last few years, ribbon width has increased from 1 to 2.5 cm, with 5 cm expected in the near-future. This factor-of-5 improvement is one reason for projecting 25 cm

TABLE V. 1980 Technology Projection and Estimated Probability Matrix

Item No.	Present	Near-Future	Future	Limit	Probability		
1	.00	1.00	1.00	1.00	1.00	1.00	1.00
2	2.50	5.00	10.00	25.00	.05	.65	.30
3	38.00	40.00	50.00	60.00	.20	.60	.20
4	.30	.20	.15	.10	.25	.60	.15
5	70.00	80.00	90.00	95.00	.40	.50	.10
6	50000.00	25000.00	20000.00	15000.00	.60	.30	.10
7	7.00	8.00	10.00	12.00	.10	.60	.30
8	.00	10.00	10.00	10.00	1.00	1.00	1.00
9	70.00	80.00	90.00	95.00	.40	.50	.10
10	.00	.05	.05	.05	1.00	1.00	1.00
11	.00	25000.00	25000.00	25000.00	1.00	1.00	1.00
12	.00	.10	.10	.10	1.00	1.00	1.00
13	.00	20000.00	20000.00	20000.00	1.00	1.00	1.00
14	.50	.25	.15	.10	.30	.60	.10
15	.00	10000.00	10000.00	10000.00	1.00	1.00	1.00
16	65.00	45.00	30.00	6.00	.60	.30	.10
17	80.00	85.00	90.00	95.00	.35	.60	.05
18	30.00	25.00	20.00	10.00	.15	.50	.35
19	.00	.05	.05	.05	1.00	1.00	1.00
20	12.00	11.00	10.00	9.00	.20	.60	.20
21	.00	50.00	50.00	50.00	1.00	1.00	1.00
22	.00	10.00	10.00	10.00	1.00	1.00	1.00
23	.00	10.00	10.00	10.00	1.00	1.00	1.00
24	.00	10.00	10.00	10.00	1.00	1.00	1.00
25	.00	168.00	168.00	168.00	1.00	1.00	1.00
26	8.00	10.00	12.00	15.00	.30	.40	.30
27	.00	1.00	1.00	1.00	1.00	1.00	1.00

TABLE VI. 1985 Technology Projection and Estimated Probability Matrix

Item No.	Present	Near-Future	Future	Limit	Probability		
1	.00	1.00	1.00	1.00	1.00	1.00	1.00
2	2.50	5.00	10.00	25.00	.02	.28	.70
3	30.00	40.00	50.00	60.00	.10	.40	.50
4	.30	.20	.15	.10	.10	.60	.30
5	70.00	80.00	90.00	95.00	.10	.65	.25
6	50000.00	25000.00	20000.00	15000.00	.05	.70	.25
7	7.00	8.00	10.00	12.00	.10	.30	.60
8	.00	10.00	10.00	10.00	1.00	1.00	1.00
9	70.00	80.00	90.00	95.00	.10	.60	.30
10	.00	.05	.05	.05	1.00	1.00	1.00
11	.00	25000.00	25000.00	25000.00	1.00	1.00	1.00
12	.00	.10	.10	.10	1.00	1.00	1.00
13	.00	20000.00	20000.00	20000.00	1.00	1.00	1.00
14	.50	.25	.15	.10	.10	.60	.30
15	.00	10000.00	10000.00	10000.00	1.00	1.00	1.00
16	65.00	45.00	30.00	6.00	.10	.50	.40
17	80.00	85.00	90.00	95.00	.10	.60	.30
18	30.00	25.00	20.00	10.00	.10	.40	.50
19	.00	.05	.05	.05	1.00	1.00	1.00
20	12.00	11.00	10.00	9.00	.10	.30	.60
21	.00	50.00	50.00	50.00	1.00	1.00	1.00
22	.00	10.00	10.00	10.00	1.00	1.00	1.00
23	.00	10.00	10.00	10.00	1.00	1.00	1.00
24	.00	10.00	10.00	10.00	1.00	1.00	1.00
25	.00	168.00	168.00	168.00	1.00	1.00	1.00
26	8.00	10.00	12.00	15.00	.05	.35	.60
27	.00	1.00	1.00	1.00	1.00	1.00	1.00

as the width limit and reflecting a reasonably high degree of confidence (0.65 probability) that, by 1980, the width will be somewhere between 5 and 10 cm. Our current projection for 1985 is that the probability is good (0.70) that silicon sheets between 10 and 25 cm wide will be pulled.

Doubling the growth rate from 30 to 60%, and, at the same time, reducing thickness to 0.10 mm, still represents a formidable, yet not impossible, challenge. This is also reflected in the estimated lower probabilities for growth rate (1980: 0.2 0.6 0.2; 1985: 0.1 0.4 0.5). Yield (items 5 and 17) and equipment availability (item 9) are difficult to project from laboratory conditions, but, from our experience in semiconductor manufacturing, tend to require diligent engineering effort, rather than technology breakthroughs, to improve. This is the basis for our optimistic outlook.

Future silicon-sheet pullers are envisioned as mass-produced ($\sim$\$20,000), special-purpose machines, highly reliable with automatic melt replenishment, and capable of near-unattended growth. If equipment meeting these conditions does not become available, perhaps because of insufficient demand for solar-cell products, then the outlook for photovoltaics should be reassessed.

4.4 Computer Evaluation

With the method described in section 3, the production-unit computer model was iterated 600 times for each of the two years (1980, 1985). Each time, from a different set of input variables, energy-capacity cost at the level of sheet material was computed. Three of the 600 sets of input variables for 1980, which resulted in the highest ($2492/kWE) and two lowest-cost ($203/kWE and $96/kWE) figures, are listed in Fig. 9. The result of calculation and of the subsequent statistical analysis can be seen in Tables VII and VIII. Similar information for 1985 is shown in Fig. 10 and Tables IX and X.

```
  RIBBON DATA FROM SIMULATIONS   DATED 11/04/75
1  RIBBONS GROWN SIMULTANEOUSLY -     1    1    1
2  RIBBON WIDTH, CM -    2.8 21.6 22.8
3  RIBBON GROWTH RATE,M/HR -    2.81  2.28  4.98 ..OR AS PCT  33  36  89
4  RIBBON THICKNESS, MM -    0.21 0.19 0.11
5  YIELD OF  CELL QUALITY  RIBBON, PCT -   86  89  73

  DIRECT COST
6  RIBBON FURNACE, DOLLARS -   38321  41821  39878
7     EQUIPMENT LIFE, YEARS -   10.0  9.1 11.2
8     INTEREST RATE, PERCENT -   16.0 10.0 10.0
9     EQUIPMENT AVAILABILITY, PERCENT -    73   79   83
   PERSONNEL PER SHIFT PER MACHINE
10 11 NO. OF SUPVS -   0.06 0.05 0.05 AT $ -  25000 25000 25000
12 13 NO. OF ENGRS -   0.10 0.10 0.10 AT $ -  20000 20000 20000
14 15 NO. OF TECHN -   0.32 0.23 0.16 AT $ -  10000 10000 10000
16 POLY SILICON COST, DOLS/KG -   60    7    6
17 POLY YIELD TO RIBBON,PERCENT -   81  89  84
   SERVICES AND SUPPLIES
18    CRUCIBLE/DIE/PARTS COST PER DAY -    21  23  17 DOLLARS
19    POWER COST AT -   0.05 0.05 0.05 DOLLARS PER KWH
20    ENERGY TO OPERATE EQUIPMENT -    11  10  11 KW

21 22  O/H -   50  50  50 PCT OF PERS+   10  10  10 PCT OF RAW MATL COST
23  G_AND_A -   10  10  10 PERCENT OF DIRECT COST+OVERHEAD

24  PROFIT BEFORE TAX, PERCENT - 10 10 10 OF DC+O/H+G+A

  MISCELLANEOUS
25 WORKWEEK, HOURS -   168 168 168
26 CONVERSION EFFICIENCY, PERCENT -   11.39 12.99 13.63
27 ENERGY DENSITY AT AM1,KW/SQ M PEAK -    1   1   1
```

Fig. 9. 1980 list of input parameters resulting in the highest and two lowest energy-capacity costs.

TABLE VII. Three Sample (Highest and Two Lowest) Energy-Capacity Cost Calculations for 1980

RIBBONS GROWN SIMULTANEOUSLY	1.00	1.00	1.00
RIBBON WIDTH, CM	2.62	21.64	22.78
AVG YLD AREA GRWTH RTE,SQ M/HR	0.03	0.35	0.67
COMBINED YIELD FACTOR	0.69	0.79	0.61
DIRECT COST IN DOLS/SQ METER			
EQUIPMENT CAPITAL RECOVERY	21.31	2.47	1.07
PERSONNEL	91.76	7.97	3.58
POLY SILICON COST	43.19	3.91	2.76
SERVICES/SUPPLIES	29.43	3.12	1.39
SUBTOTAL:	185.70	17.48	8.81
OVERHEAD COST IN DOLS/SQ METER	48.06	4.38	1.96
G&A EXPENSES IN DOLS/SQ METER	23.46	2.18	1.08
PROFIT IN DOLLARS/SQ METER	25.88	2.39	1.18
TOTAL COST IN DOLS/SQ METER	283.81	26.34	13.03
DOLLARS PER KW	2491.97	282.79	95.58

TABLE VIII. Statistical Analysis of 1980 Energy-Capacity Cost Figures

Parameter	Value
Sample size	600
Maximum	2492
Minimum	96
Range	2396
Mean	769.605
Variance	105026
Standard deviation	324.078
Mean deviation	246.311
Median	725
Mode	681

```
  RIBBON DATA FROM SIMULATIONS   DATED 11/04/75
1  RIBBONS GROWN SIMULTANEOUSLY -     1    1    1
2  RIBBON WIDTH, CM -      3.3 23.6 24.8
3  RIBBON GROWTH RATE,M/HR -    2.34  2.60  5.09 ..OR AS PCT  37  40  60
4  RIBBON THICKNESS, MM -  0.15 0.17 0.11
5  YIELD OF CELL QUALITY RIBBON, PCT -   89  92  80

  DIRECT COST
6  RIBBON FURNACE, DOLLARS -   23385  23965  23621
7     EQUIPMENT LIFE, YEARS -  11.0 10.1 11.6
8     INTEREST RATE, PERCENT -  10.0 10.0 10.0
9     EQUIPMENT AVAILABILITY, PERCENT -    80   84   80
  PERSONNEL PER SHIFT PER MACHINE
10 11 NO. OF SUPVS -   0.05 0.05 0.05 AT $ -  25000 25000 25000
12 13 NO. OF ENGRS -   0.10 0.10 0.10 AT $ -  20000 20000 20000
14 15 NO. OF TECHN -   0.23 0.20 0.12 AT $ -  10000 10000 10000
16 POLY SILICON COST, DOLS/KG -   64    7    6
17 POLY YIELD TO RIBBON,PERCENT -   83   92   87
  SERVICES AND SUPPLIES
18    CRUCIBLE/DIE/PARTS COST PER DAY -   20  22  15 DOLLARS
19    POWER COST AT -   0.05 0.05 0.05 DOLLARS PER KWH
20    ENERGY TO OPERATE EQUIPMENT -   10  10  10 KW

21 22  O/H -   50  50  50 PCT OF PERS+   10  10  10 PCT OF RAW MATL COST
23  G AND A -   10  10  10 PERCENT OF DIRECT COST+OVERHEAD

24  PROFIT BEFORE TAX, PERCENT - 10 10 10 OF DC+O/H+G+A

  MISCELLANEOUS
25 WORKWEEK, HOURS -  168 168 168
26 CONVERSION EFFICIENCY, PERCENT -  12.89 14.00 14.32
27 ENERGY DENSITY AT AM1,KW/SQ M PEAK -    1    1    1
```

Fig. 10. 1985 list of input parameters resulting in the highest and two lowest energy-capacity costs.

TABLE IX. Three Sample (Highest and Two Lowest) Energy-Capacity Cost Calculations for 1985

RIBBONS GROWN SIMULTANEOUSLY	1.00	1.00	1.00
RIBBON WIDTH, CM	3.29	23.56	24.05
AVG YLD AREA GRWTH RTE,SQ M/HR	0.05	0.49	0.06
COMBINED YIELD FACTOR	0.73	0.85	0.69
DIRECT COST IN DOLS/SQ METER			
EQUIPMENT CAPITAL RECOVERY	7.86	0.94	0.49
PERSONNEL	50.81	5.32	2.62
POLY SILICON COST	32.94	3.48	2.29
SERVICES/SUPPLIES	10.29	2.14	1.01
SUBTOTAL:	109.91	11.81	6.42
OVERHEAD COST IN DOLS/SQ METER	27.82	2.96	1.47
G+A EXPENSES IN DOLS/SQ METER	13.77	1.48	0.79
PROFIT IN DOLLARS/SQ METER	15.15	1.62	0.87
TOTAL COST IN DOLS/SQ METER	166.65	17.86	9.54
DOLLARS PER KW	1292.98	127.56	66.66

TABLE X. Statistical Analysis of 1985 Energy-Capacity Cost Figures

Parameter	Value
Sample size	600
Maximum	1293
Minimum	67
Range	1226
Mean	413.728
Variance	29022
Standard deviation	170.358
Mean deviation	128.373
Median	385
Mode	410

Accordingly, an energy-capacity cost for 1980 of $750/kWE is projected, which is between the mean ($770/kWE) and the median ($725/kWE). For 1985, the projected value is $350/kWE, derived from the mean ($414/kWE), the median ($385/kWE), and subsequent iterations. To confirm the results, the procedure was iterated another 600 times, each time with a different stream of random numbers. The statistical analysis resulted, for 1980, in a mean of $778/kWE and a median of $727/kWE. For 1985, the values were $369/kWE and $342/kWE, respectively, or about 10% lower than the first set.

Figure 11 shows the frequency distributions of these four sets of 600 energy-capacity costs. It is noted that the

1985 distributions are grouped considerably tighter around the median, perhaps because our probability estimates have less variation for that later point in time.

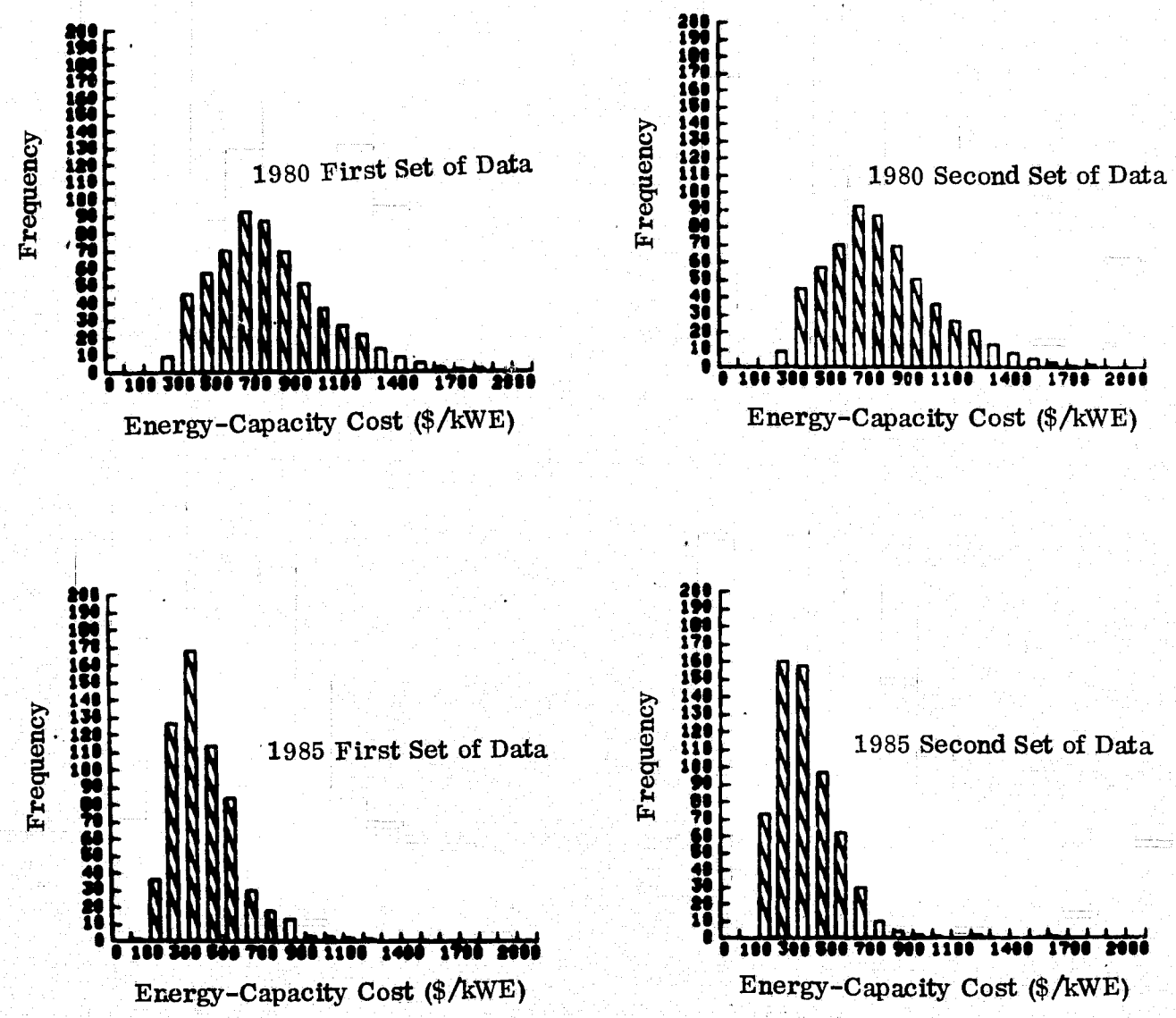

Fig. 11. Frequency distribution of calculated energy-capacity costs.

At JPL's suggestion, a further statistical test was performed, again using a different random number seed, primarily to confirm that a steady state had been reached. The result of the 1985 calculation, shown in Table XI, confirmed this condition. As shown, 2223 calculations were performed (first column) before the APL workspace was full, and calculation was terminated. Intermediate results were printed every 60 lines. The second column shows the mean, the third the median, and the last three the standard deviation, the mean deviation, and the remaining workspace size.

TABLE XI. Statistical Analysis of 1985 Energy-Capacity Cost Figures, Including Iterations

Iteration	Mean	Median	Standard Deviation	Mean Deviation	AWA
3	284	269	122	86	45204
63	369	343	146	119	44724
123	363	347	130	102	44244
183	359	347	128	101	43764
243	353	335	130	103	43284
303	355	332	143	108	42804
363	353	331	138	105	42324
423	351	330	141	107	41844
483	355	334	147	111	41364
543	360	337	153	114	40884
603	359	338	152	114	40404
663	362	342	155	117	39924
723	361	340	155	117	39444
783	361	339	153	116	38964
843	362	340	152	116	38484
903	361	338	155	117	38004
963	362	340	154	117	37524
1023	363	339	156	118	37044
1083	362	336	156	118	36564
1143	363	336	159	120	36084
1203	362	336	158	120	35604
1263	363	336	160	121	35124
1323	364	338	160	121	34644
1383	362	335	159	121	34164
1443	363	335	159	120	33684
1503	363	336	158	119	33204
1563	363	336	157	119	32724
1623	363	337	157	119	32244
1683	364	338	157	119	31764
1743	363	338	156	118	31284
1803	364	338	156	118	30804
1863	365	339	156	118	30324
1923	366	339	157	119	29844
1983	365	340	156	118	29364
2043	365	341	156	118	28884
2103	365	341	155	118	28404
2163	365	340	156	118	27924
2223	365	340	157	118	27444

4.5 Analysis of Results

An important consideration is whether or not this "bottoms-up" process-related analysis supports the projections of future energy-capacity cost arrived at by other means. To analyze this further, ERDA-projected (4) "established silicon array costs" are plotted together with the results of this study in Fig. 12, where both a regular plot and a log plot are shown.

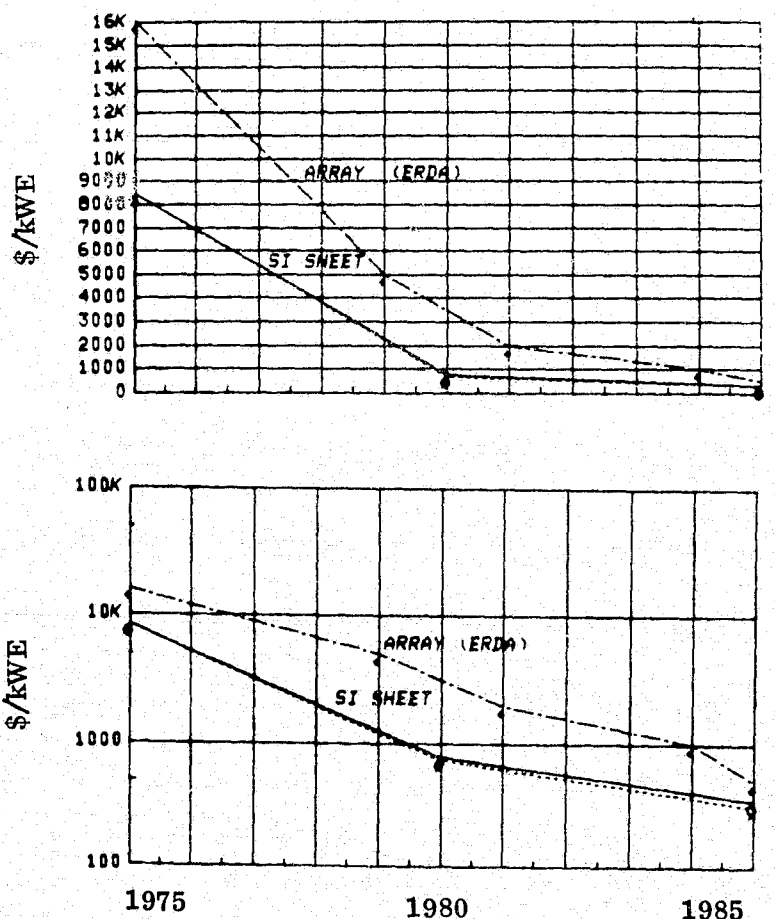

Fig. 12. Plot and log plot of projected silicon-sheet material and array cost versus time.

Generally speaking, the value of single-crystal silicon material should not exceed 30% of array cost. For the remainder of this decade, as can be seen from Fig. 12, our projection of energy-capacity cost at the silicon-sheet material level is somewhat less than half of the array cost projected by ERDA and thus within the accuracy level of this type of projection. From 1980 through 1985, however, this band narrows to a point in 1985 where projected energy-capacity cost at the level of sheet material ($350/kWE) almost equals array cost ($500/kWE).

In sum, it is concluded that compatibility and general agreement exist between this study and ERDA projections, particularly through 1980.

5. CONCLUSIONS

A new technology forecasting technique is being developed and applied to projecting the future cost of energy at the level of silicon-sheet material. This technique is based upon the production-unit concept and deals with the economics of material manufacturing from a processing parameter, or "bottoms up," standpoint. From a baseline, or state-of-the-art, future technology capability is projected through full maturity.

The concept of chronology is introduced by estimating the probability of meeting the objective associated with the technology parameter at a stated point in time. From this probability density function, the cumulative probability distribution function is derived. The latter function is evaluated numerically, thus providing a set of input parameters to the production-unit model. Calculation, followed by subsequent iteration of this procedure, and final statistical analysis of the accumulated output from the model form the basis for the projected energy-capacity cost versus time relationship.

Application of this technique results in the following outlook for large-area silicon sheets:

- Silicon-sheet technology has the potential for achieving future low-cost material objectives for photovoltaic applications, if development milestones defined in this study are met.

- 1980 and 1985 energy-capacity costs of $750/kWE and $350/kWE, respectively, at the level of silicon-sheet material, are projected.

- This analysis confirms, from a silicon-sheet material standpoint, that ERDA-stated

energy-capacity cost objectives at the array level are achievable. However, there appears to be little, if any, margin for error.

- Through 1980, a factor of ∿2 difference exists between ERDA-projected costs at the array level and our cost at the silicon-sheet material level. By 1985, this difference has essentially disappeared ($500/kWE and $350/kWE), which is an undesirable cost trend requiring further analysis.

6. REFERENCES

1. Quarterly Technical Progress Report Number 2, JPL Contract 954144, G. H. Schwuttke, Principal Investigator, December 15, 1975.

2. Geoffrey Gordon, System Simulation, Prentice-Hall, Inc., New Jersey (1969).

3. Quarterly Technical Progress Report Number 3, JPL Contract 954144, G. H. Schwuttke, Principal Investigator, March 15, 1976.

4. Proceedings of the First ERDA Semiannual Solar Photovoltaic Conversion Program Conference, p. 11, UCLA, July 22-25, 1975.

FIFTH QUARTER ACTIVITY PLAN

- Continue process studies on ribbon perfection.
- Optimize 38-mm-wide ribbon growth.
- Study influence of ribbon defects on lifetime and solar-cell efficiency.
- Continue work on comparative analysis of material-area throughput capability between capillary action shaping technique and Czochralski processing, using computer graphics.
- Expand ribbon-growth computer model to address other material-processing steps.